Homogenization of woven materials

Rikte, Sten; Andersson, Michael; Kristensson, Gerhard

1998

CODEN:LUTEDX/(TEAT-7074)/1-33/(1998)
Revision No. 1: September 1999

Homogenization of woven materials

Sten Rikte, Michael Andersson, and Gerhard Kristensson

Department of Electroscience
Electromagnetic Theory
Lund Institute of Technology
Sweden

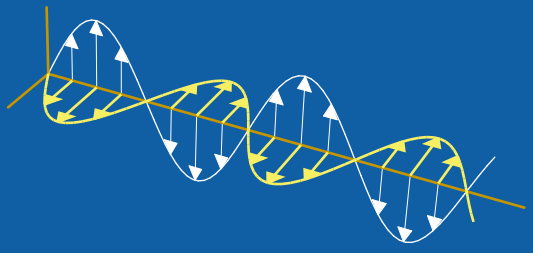

Sten Rikte, Michael Andersson, and Gerhard Kristensson

Department of Electroscience
Electromagnetic Theory
Lund Institute of Technology
P.O. Box 118
SE-221 00 Lund
Sweden

Editor: Gerhard Kristensson

Abstract

The effective electric and magnetic material properties of a complex (two-component) mixture are addressed. The mixture is periodic in two directions and has a finite thickness in the third direction. Specifically, the explicit problem of finding the effective electric parameters for slab that has been reinforced by a layer (or several layers) of glass fiber is investigated. The homogenization problem is solved by a series expansion (multiple-scale technique), and the numerical solution of the two-dimensional vector-valued problem is found by a FEM formulation. The FEM problem is non-standard due to the periodic boundary conditions of the problem. Several numerical computations show that the most important parameter of the effective permittivity is the volume fraction of the guest material in the host. The reflection and transmission properties of the homogenized material are also addressed.

1 Introduction

New materials with complex electric and magnetic properties are constantly introduced in the engineering sciences. Some of these materials consist of mixtures of materials with different electric or magnetic properties, and usually the size of the mixture components is small in some sense, *e.g.*, the size or the periodicity, compared to the wavelength. Such problems call for accurate homogenization procedures, since the problem is too complex to be solved in detail. The basic mathematical aspects of homogenization are found in the literature. Classical mathematical references in this field are Ref. 3, 23, 24.

In the electrical engineering sciences, the homogenization problem amounts to finding the effective electrical and magnetic parameters of the mixture. This topic has a vast literature, and we have no intention in this paper to review this field. However, the recent papers by Kuester and Holloway [15–17], who use a procedure similar to the one adopted in this paper, are of interest.

This paper deals with the fundamental topic of finding the effective electric and magnetic parameters of a two (or several) component mixture. The mixture is periodic in two directions and has a finite thickness in the third direction. Specifically, the explicit problem of finding the effective electric parameters for a slab that has been reinforced by a layer (or several layers) of glass fiber is of primary interest. The geometry of a typical example is depicted in Figure 1. Very few references address this geometry [4]. This particular geometry has important applications in radome technology [14], but also in penetration of microwave radiation in woven materials and in printed circuit technology [1]. The woven materials are also of interest in thermal conductivity problems [10, 11, 19, 20].

In Section 2, the basic equations for the homogenization problem are introduced. The main result of this section is that electrostatic problems with periodic boundary conditions have to be solved. The numerical solution of this problem is addressed in Section 3. This problem is solved by the finite element method (FEM). The numerical results are presented in Section 4. The dynamics of the average field, the homogenization of a thin uniaxial slab and reflection and its transmission properties

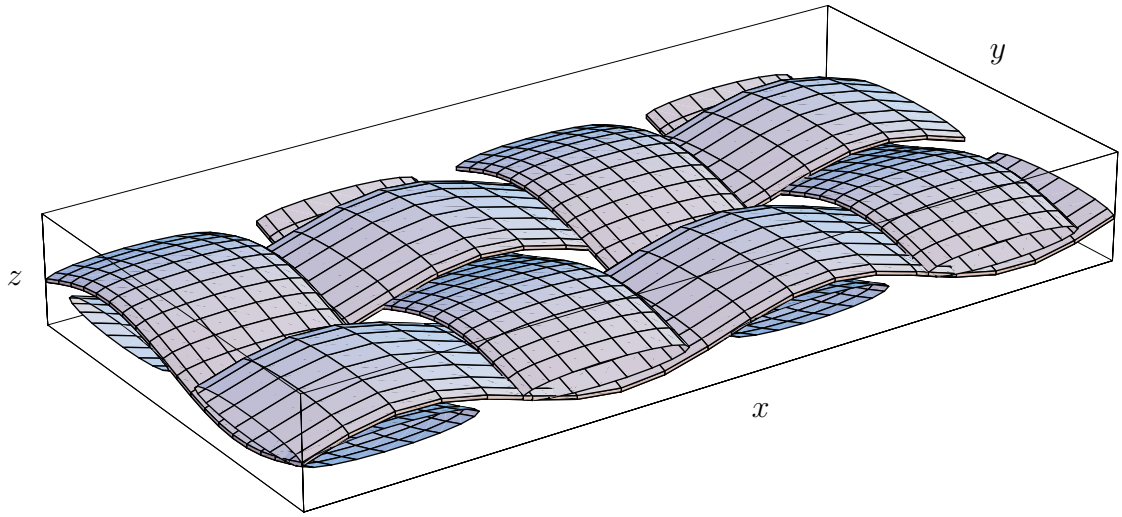

Figure 1: The geometry of the glass fiber.

are investigated in Section 5. The appropriate edge element functions of the FEM analysis and the technical details of numerical analysis are collected in a series of appendices at the end of the paper.

2 The homogenization scheme

Throughout this paper, scalars are typed in italic letters, vectors in italic boldface, and dyadics in roman boldface, respectively. The position vector is denoted by $\boldsymbol{r} = \hat{\boldsymbol{x}}x + \hat{\boldsymbol{y}}y + \hat{\boldsymbol{z}}z$, where $\hat{\boldsymbol{x}}$, $\hat{\boldsymbol{y}}$, and $\hat{\boldsymbol{z}}$ are the Cartesian basis vectors.

The permittivity and the permeability functions are assumed to be periodic in the x- and y-variables, *i.e.*,

$$\begin{cases} \epsilon(\boldsymbol{r} + mp_x\hat{\boldsymbol{x}} + np_y\hat{\boldsymbol{y}}, \omega) = \epsilon(\boldsymbol{r}, \omega) \\ \mu(\boldsymbol{r} + mp_x\hat{\boldsymbol{x}} + np_y\hat{\boldsymbol{y}}, \omega) = \mu(\boldsymbol{r}, \omega) \end{cases}$$

The variation in the transverse direction has length scale $p = \max\{p_x, p_y\}$, which is small, *i.e.*, the microscopic length scale[1]. The macroscopic length scale[2] over which the fields varies is l, which we assume to be large compared to p, *i.e.*, $l \gg p$.

The electric and the magnetic fields $\boldsymbol{E}$ and $\boldsymbol{H}$, respectively, satisfy the Maxwell equations

$$\begin{cases} \nabla \times \boldsymbol{E}(\boldsymbol{r}, \omega) = i\omega\mu(\boldsymbol{r}, \omega)\boldsymbol{H}(\boldsymbol{r}, \omega) \\ \nabla \times \boldsymbol{H}(\boldsymbol{r}, \omega) = -i\omega\epsilon(\boldsymbol{r}, \omega)\boldsymbol{E}(\boldsymbol{r}, \omega) \end{cases}$$

We apply a multiple-scale representation for the fields $\boldsymbol{E}$ and $\boldsymbol{H}$ [16, 17]. The slow variation is described by the variable $\boldsymbol{r}$ and the fast transverse variation by $\boldsymbol{\xi}$, which

[1]We assume that both p_x and p_y are finite.

[2]In Section 5, a plane wave expansion of the fields is made. Using the notation of Section 5, we naturally associate l with the transverse wave number, k_t, of such an expansion, *i.e.*, $l = 2\pi/k_t$.

are normalized $\boldsymbol{\xi} = (x\hat{\boldsymbol{x}} + y\hat{\boldsymbol{y}})/p$.

$$\begin{cases} \boldsymbol{E}(\boldsymbol{r}) = \boldsymbol{E}(\boldsymbol{r}, \boldsymbol{\xi}) \\ \boldsymbol{H}(\boldsymbol{r}) = \boldsymbol{H}(\boldsymbol{r}, \boldsymbol{\xi}) \end{cases}$$

The gradient operator then becomes

$$\nabla = \nabla_{\boldsymbol{r}} + \frac{1}{p}\nabla_{\boldsymbol{\xi}}$$

The Maxwell equations become

$$\begin{cases} \frac{1}{p}\nabla_{\boldsymbol{\xi}} \times \boldsymbol{E}(\boldsymbol{r}, \boldsymbol{\xi}) + \nabla_{\boldsymbol{r}} \times \boldsymbol{E}(\boldsymbol{r}, \boldsymbol{\xi}) = i\omega\mu(z, \boldsymbol{\xi})\boldsymbol{H}(\boldsymbol{r}, \boldsymbol{\xi}) \\ \frac{1}{p}\nabla_{\boldsymbol{\xi}} \times \boldsymbol{H}(\boldsymbol{r}, \boldsymbol{\xi}) + \nabla_{\boldsymbol{r}} \times \boldsymbol{H}(\boldsymbol{r}, \boldsymbol{\xi}) = -i\omega\epsilon(z, \boldsymbol{\xi})\boldsymbol{E}(\boldsymbol{r}, \boldsymbol{\xi}) \end{cases}$$

where $\epsilon(z, \boldsymbol{\xi}) = \epsilon(\boldsymbol{r})$ and $\mu(z, \boldsymbol{\xi}) = \mu(\boldsymbol{r})$. We expand the fields in a power series in p, *i.e.*,

$$\begin{cases} \boldsymbol{E}(\boldsymbol{r}, \boldsymbol{\xi}) = \boldsymbol{E}_0(\boldsymbol{r}, \boldsymbol{\xi}) + \boldsymbol{E}_1(\boldsymbol{r}, \boldsymbol{\xi})p + \boldsymbol{E}_2(\boldsymbol{r}, \boldsymbol{\xi})p^2 + \dots \\ \boldsymbol{H}(\boldsymbol{r}, \boldsymbol{\xi}) = \boldsymbol{H}_0(\boldsymbol{r}, \boldsymbol{\xi}) + \boldsymbol{H}_1(\boldsymbol{r}, \boldsymbol{\xi})p + \boldsymbol{H}_2(\boldsymbol{r}, \boldsymbol{\xi})p^2 + \dots \end{cases}$$

where $\boldsymbol{E}_k$ and $\boldsymbol{H}_k$ are periodic in $\boldsymbol{\xi}$:

$$\begin{cases} \boldsymbol{E}_k(\boldsymbol{r}, \boldsymbol{\xi} + mp_x\hat{\boldsymbol{x}} + np_y\hat{\boldsymbol{y}}) = \boldsymbol{E}_k(\boldsymbol{r}, \boldsymbol{\xi}) \\ \boldsymbol{H}_k(\boldsymbol{r}, \boldsymbol{\xi} + mp_x\hat{\boldsymbol{x}} + np_y\hat{\boldsymbol{y}}) = \boldsymbol{H}_k(\boldsymbol{r}, \boldsymbol{\xi}) \end{cases} \qquad k = 0, 1, 2, \dots \tag{2.1}$$

Insert this expansion in the Maxwell equations and identify different powers of p. The lowest power (p^{-1}) is :

$$\begin{cases} \nabla_{\boldsymbol{\xi}} \times \boldsymbol{E}_0(\boldsymbol{r}, \boldsymbol{\xi}) = \boldsymbol{0} \\ \nabla_{\boldsymbol{\xi}} \times \boldsymbol{H}_0(\boldsymbol{r}, \boldsymbol{\xi}) = \boldsymbol{0} \end{cases}$$

and for (p^k, $k = 0, 1, 2, \dots$)

$$\begin{cases} \nabla_{\boldsymbol{\xi}} \times \boldsymbol{E}_{k+1}(\boldsymbol{r}, \boldsymbol{\xi}) = -\nabla_{\boldsymbol{r}} \times \boldsymbol{E}_k(\boldsymbol{r}, \boldsymbol{\xi}) + i\omega\mu(z, \boldsymbol{\xi})\boldsymbol{H}_k(\boldsymbol{r}, \boldsymbol{\xi}) \\ \nabla_{\boldsymbol{\xi}} \times \boldsymbol{H}_{k+1}(\boldsymbol{r}, \boldsymbol{\xi}) = -\nabla_{\boldsymbol{r}} \times \boldsymbol{H}_k(\boldsymbol{r}, \boldsymbol{\xi}) - i\omega\epsilon(z, \boldsymbol{\xi})\boldsymbol{E}_k(\boldsymbol{r}, \boldsymbol{\xi}) \end{cases} \tag{2.2}$$

We see that the lowest power contribution is determined by the solution of a two-dimensional static problem. This static problem is identified by taking the divergence of both sides of the Maxwell equations, *i.e.*,

$$\begin{cases} \frac{1}{p}\nabla_{\boldsymbol{\xi}} \cdot (\epsilon(z, \boldsymbol{\xi})\boldsymbol{E}(\boldsymbol{r}, \boldsymbol{\xi})) = -\nabla_{\boldsymbol{r}} \cdot (\epsilon(z, \boldsymbol{\xi})\boldsymbol{E}(\boldsymbol{r}, \boldsymbol{\xi})) \\ \frac{1}{p}\nabla_{\boldsymbol{\xi}} \cdot (\mu(z, \boldsymbol{\xi})\boldsymbol{H}(\boldsymbol{r}, \boldsymbol{\xi})) = -\nabla_{\boldsymbol{r}} \cdot (\mu(z, \boldsymbol{\xi})\boldsymbol{H}(\boldsymbol{r}, \boldsymbol{\xi})) \end{cases}$$

and an identification of powers of p gives

$$p^{-1}: \qquad \begin{cases} \nabla_{\boldsymbol{\xi}} \cdot (\epsilon(z,\boldsymbol{\xi})\boldsymbol{E}_0(\boldsymbol{r},\boldsymbol{\xi})) = 0 \\ \nabla_{\boldsymbol{\xi}} \cdot (\mu(z,\boldsymbol{\xi})\boldsymbol{H}_0(\boldsymbol{r},\boldsymbol{\xi})) = 0 \end{cases}$$

and

$$p^{k}: \qquad \begin{cases} \nabla_{\boldsymbol{\xi}} \cdot (\epsilon(z,\boldsymbol{\xi})\boldsymbol{E}_{k+1}(\boldsymbol{r},\boldsymbol{\xi})) = -\nabla_{\boldsymbol{r}} \cdot (\epsilon(z,\boldsymbol{\xi})\boldsymbol{E}_k(\boldsymbol{r},\boldsymbol{\xi})) \\ \nabla_{\boldsymbol{\xi}} \cdot (\mu(z,\boldsymbol{\xi})\boldsymbol{H}_{k+1}(\boldsymbol{r},\boldsymbol{\xi})) = -\nabla_{\boldsymbol{r}} \cdot (\mu(z,\boldsymbol{\xi})\boldsymbol{H}_k(\boldsymbol{r},\boldsymbol{\xi})) \end{cases} \qquad k = 0, 1, 2, \ldots$$

A lowest-order approximation to the propagation problem is obtained by first averaging (2.2) for $k = 0$ over a unit cell. Owing to Gauss' theorem and the periodicity condition (2.1), one gets

$$\begin{cases} \nabla_{\boldsymbol{r}} \times <\boldsymbol{E}_0(\boldsymbol{r},\boldsymbol{\xi})> = i\omega <\mu(z,\boldsymbol{\xi})\boldsymbol{H}_0(\boldsymbol{r},\boldsymbol{\xi})> \\ \nabla_{\boldsymbol{r}} \times <\boldsymbol{H}_0(\boldsymbol{r},\boldsymbol{\xi})> = -i\omega <\epsilon(z,\boldsymbol{\xi})\boldsymbol{E}_0(\boldsymbol{r},\boldsymbol{\xi})> \end{cases}$$

where the average values, denoted by $<\cdot>$, are defined in subsection 2.1. The resulting equations

$$\begin{cases} \nabla_{\boldsymbol{r}} \times <\boldsymbol{E}_0>(\boldsymbol{r}) = i\omega \boldsymbol{\mu}_{\text{eff}}(z) \cdot <\boldsymbol{H}_0>(\boldsymbol{r}) \\ \nabla_{\boldsymbol{r}} \times <\boldsymbol{H}_0>(\boldsymbol{r}) = -i\omega \boldsymbol{\epsilon}_{\text{eff}}(z) \cdot <\boldsymbol{E}_0>(\boldsymbol{r}) \end{cases} \tag{2.3}$$

can then be solved using standard methods, see Section 5. The homogenized permittivity and permeability dyadics, $\boldsymbol{\epsilon}_{\text{eff}}(z)$ and $\boldsymbol{\mu}_{\text{eff}}(z)$, respectively, are here dependent on the depth parameter z.

2.1 Definition of effective parameters

We introduce an average operator $<\cdot>$ defined by

$$<f>(\boldsymbol{r}) = \iint_{\Omega} f(\boldsymbol{r},\boldsymbol{\xi})\, d\xi_x\, d\xi_y$$

where Ω is a periodic unit cell (a rectangle).

The homogenized (effective) permittivity dyadic, $\boldsymbol{\epsilon}_{\text{eff}}(z)$, and permeability dyadic, $\boldsymbol{\mu}_{\text{eff}}(z)$, are defined as

$$\begin{cases} <\epsilon(z,\boldsymbol{\xi})\boldsymbol{E}_0(\boldsymbol{r},\boldsymbol{\xi})> = \boldsymbol{\epsilon}_{\text{eff}}(z) \cdot <\boldsymbol{E}_0(\boldsymbol{r},\boldsymbol{\xi})> \\ <\mu(z,\boldsymbol{\xi})\boldsymbol{H}_0(\boldsymbol{r},\boldsymbol{\xi})> = \boldsymbol{\mu}_{\text{eff}}(z) \cdot <\boldsymbol{H}_0(\boldsymbol{r},\boldsymbol{\xi})> \end{cases}$$

In subsection 2.2 below, we argue that the effective permittivity and permeability dyadics for the inhomogeneous isotropic medium, are of the form (an anisotropic medium)

$$\begin{cases} \boldsymbol{\epsilon}_{\text{eff}}(z) = \boldsymbol{\epsilon}_{\text{eff},\perp\perp}(z) + \hat{\boldsymbol{z}}\hat{\boldsymbol{z}}\epsilon_{\text{eff},zz}(z) \\ \boldsymbol{\mu}_{\text{eff}}(z) = \boldsymbol{\mu}_{\text{eff},\perp\perp}(z) + \hat{\boldsymbol{z}}\hat{\boldsymbol{z}}\mu_{\text{eff},zz}(z) \end{cases} \tag{2.4}$$

where

$$\begin{cases} \boldsymbol{\epsilon}_{\text{eff},\perp\perp}(z) = \hat{\boldsymbol{x}}\hat{\boldsymbol{x}}\epsilon_{\text{eff},xx}(z) + \hat{\boldsymbol{x}}\hat{\boldsymbol{y}}\epsilon_{\text{eff},xy}(z) + \hat{\boldsymbol{y}}\hat{\boldsymbol{x}}\epsilon_{\text{eff},yx}(z) + \hat{\boldsymbol{y}}\hat{\boldsymbol{y}}\epsilon_{\text{eff},yy}(z) \\ \boldsymbol{\mu}_{\text{eff},\perp\perp}(z) = \hat{\boldsymbol{x}}\hat{\boldsymbol{x}}\mu_{\text{eff},xx}(z) + \hat{\boldsymbol{x}}\hat{\boldsymbol{y}}\mu_{\text{eff},xy}(z) + \hat{\boldsymbol{y}}\hat{\boldsymbol{x}}\mu_{\text{eff},yx}(z) + \hat{\boldsymbol{y}}\hat{\boldsymbol{y}}\mu_{\text{eff},yy}(z) \end{cases} \tag{2.5}$$

The explicit expressions for $\epsilon_{\text{eff},zz}(z)$ and $\mu_{\text{eff},zz}(z)$ are found to be

$$\begin{cases} \epsilon_{\text{eff},zz}(z) = <\epsilon>(z)/|\Omega| \\ \mu_{\text{eff},zz}(z) = <\mu>(z)/|\Omega| \end{cases} \tag{2.6}$$

where $|\Omega|$ is the measure (area) of the unit cell Ω. No magneto-electric coupling occurs; consequently, the effective medium is not bianisotropic.

2.2 The two-dimensional, periodic, electrostatic problem

In order to obtain the effective medium parameters, we wish to solve the two-dimensional, static, one-parametric problem

$$\begin{cases} \nabla_{\boldsymbol{\xi}} \times \boldsymbol{E}_0(z, \boldsymbol{\xi}) = \boldsymbol{0} \\ \nabla_{\boldsymbol{\xi}} \cdot (\epsilon(z, \boldsymbol{\xi}) \boldsymbol{E}_0(z, \boldsymbol{\xi})) = 0 \end{cases}$$

subjected to the periodicity condition (2.1). An analogous problem has to be solved for the magnetic field.

It is appropriate to decompose the electric field into its tangential and normal components as

$$\begin{cases} \boldsymbol{E}_0(z, \boldsymbol{\xi}) = \boldsymbol{E}_{0,xy}(z, \boldsymbol{\xi}) + \hat{\boldsymbol{z}} E_{0,z}(z, \boldsymbol{\xi}) \\ \boldsymbol{E}_{0,xy}(z, \boldsymbol{\xi}) = \hat{\boldsymbol{x}} E_{0,x}(z, \boldsymbol{\xi}) + \hat{\boldsymbol{y}} E_{0,y}(z, \boldsymbol{\xi}) \end{cases}$$

The vector equation shows that there is no coupling between the normal component of the field, $E_{0,z}(z, \boldsymbol{\xi})$, and the tangential component of the field, $\boldsymbol{E}_{0,xy}(z, \boldsymbol{\xi})$, and that the normal field component is independent of $\boldsymbol{\xi}$; consequently, the principal form of the effective permittivity dyadic is, indeed, given by equations (2.4)–(2.6).

Thus, the above static problem reduces to

$$\begin{cases} \nabla_{\boldsymbol{\xi}} \times \boldsymbol{E}_{0,xy}(z, \boldsymbol{\xi}) = \boldsymbol{0} \\ \nabla_{\boldsymbol{\xi}} \cdot (\epsilon(z, \boldsymbol{\xi}) \boldsymbol{E}_{0,xy}(z, \boldsymbol{\xi})) = 0 \end{cases} \tag{2.7}$$

where

$$\boldsymbol{E}_{0,xy}(z, \boldsymbol{\xi} + mp_x\hat{\boldsymbol{x}} + np_y\hat{\boldsymbol{y}}) = \boldsymbol{E}_{0,xy}(z, \boldsymbol{\xi}) \tag{2.8}$$

and z is a parameter. It can be argued that the problem (2.7)–(2.8) has precisely

two linearly independent solutions [12, p. 219][3]. Therefore, a matrix representation of the effective permittivity dyadic $\boldsymbol{\epsilon}_{\text{eff},\perp\perp}(z)$ is

$$\begin{aligned}&\boldsymbol{\epsilon}_{\text{eff},\perp\perp}(z) = \\ &\left(<\boldsymbol{D}_{0,xy,1}(z,\boldsymbol{\xi})> \; <\boldsymbol{D}_{0,xy,2}(z,\boldsymbol{\xi})>\right) \cdot \left(<\boldsymbol{E}_{0,xy,1}(z,\boldsymbol{\xi})> \; <\boldsymbol{E}_{0,xy,2}(z,\boldsymbol{\xi})>\right)^{-1}\end{aligned} \tag{2.9}$$

where the column vectors $<\boldsymbol{E}_{0,xy,1}(z,\boldsymbol{\xi})>$ and $<\boldsymbol{E}_{0,xy,2}(z,\boldsymbol{\xi})>$ are Cartesian representations of the two linearly independent solutions to the problem (2.7)–(2.8). We illustrate this for the case of a layered structure.

2.3 Simple analytic example

Consider an isotropic medium that is periodically stratified in the x-direction. Each period is defined by n simple, isotropic layers whose permittivities and permeabilities are ϵ_i $(i = 1, \ldots, n)$ and μ_i $(i = 1, \ldots, n)$, respectively, and whose thicknesses are d_i $(i = 1, \ldots, n)$. Indeed, this medium is periodic in the x- and y-directions with the periods $p_x = \sum_{i=1}^{n} d_i$ and $p_y =$ arbitrary, respectively. Two linearly independent solutions to the problem (2.7)–(2.8) are

1. $\boldsymbol{D}_{0,xy}(z,\boldsymbol{\xi}) = \hat{\boldsymbol{x}} D$, where D is a constant, and
2. $\boldsymbol{E}_{0,xy}(z,\boldsymbol{\xi}) = \hat{\boldsymbol{y}} E$, where E is a constant,

and $\boldsymbol{D}_{0,xy}(z,\boldsymbol{\xi}) = \hat{\boldsymbol{x}} D_{0,x}(z,\boldsymbol{\xi}) + \hat{\boldsymbol{y}} D_{0,y}(z,\boldsymbol{\xi}) = \epsilon(\boldsymbol{\xi})\boldsymbol{E}_{0,xy}(z,\boldsymbol{\xi})$ denotes the tangential electric flux density. Thus, by definition, the effective medium parameters are

$$\begin{cases} \epsilon_{\text{eff},xx} = \dfrac{<D_{0,x}>}{<E_{0,x}>} = \dfrac{p_x}{\sum_{i=1}^{n} d_i/\epsilon_i} \\ \epsilon_{\text{eff},xy} = \dfrac{<D_{0,x}>}{<E_{0,y}>} = \epsilon_{\text{eff},yx} = \dfrac{<D_{0,y}>}{<E_{0,x}>} = 0 \\ \epsilon_{\text{eff},yy} = \dfrac{<D_{0,y}>}{<E_{0,y}>} = \dfrac{\sum_{i=1}^{n} d_i\epsilon_i}{p_x} = \epsilon_{\text{eff},zz} \end{cases}$$

As expected, the effective medium is a homogeneous, uniaxial material with the optical axis in the x-direction:

$$\boldsymbol{\epsilon}_{\text{eff}} = \hat{\boldsymbol{x}}\hat{\boldsymbol{x}} \frac{\sum_{i=1}^{n} d_i}{\sum_{i=1}^{n} d_i/\epsilon_i} + (\hat{\boldsymbol{y}}\hat{\boldsymbol{y}} + \hat{\boldsymbol{z}}\hat{\boldsymbol{z}}) \frac{\sum_{i=1}^{n} d_i\epsilon_i}{\sum_{i=1}^{n} d_i} \tag{2.10}$$

Analogously,

$$\boldsymbol{\mu}_{\text{eff}} = \hat{\boldsymbol{x}}\hat{\boldsymbol{x}} \frac{\sum_{i=1}^{n} d_i}{\sum_{i=1}^{n} d_i/\mu_i} + (\hat{\boldsymbol{y}}\hat{\boldsymbol{y}} + \hat{\boldsymbol{z}}\hat{\boldsymbol{z}}) \frac{\sum_{i=1}^{n} d_i\mu_i}{\sum_{i=1}^{n} d_i}$$

[3]It is easy to see that there are no classical solutions of the form $\boldsymbol{E}_{0,xy} = -\nabla_{\boldsymbol{\xi}}\phi$, but $\phi =$ constant, if we require that ϕ and $\nabla_{\boldsymbol{\xi}}\phi$ are periodic and smooth functions in the $\boldsymbol{\xi}$-variable. Apply the divergence theorem over the unit cell Ω and use the periodicity. We get

$$\iint_{\Omega} \epsilon \left|\nabla_{\boldsymbol{\xi}}\phi\right|^2 \, d\xi_x \, d\xi_y = \iint_{\Omega} \nabla_{\boldsymbol{\xi}} \cdot (\phi\epsilon\nabla_{\boldsymbol{\xi}}\phi) \, d\xi_x \, d\xi_y = \int_{\delta\Omega} \hat{\boldsymbol{\nu}} \cdot (\phi\epsilon\nabla_{\boldsymbol{\xi}}\phi) \, dl = 0$$

This implies, provided $\epsilon \neq 0$, that $\phi =$ constant.

2.4 Weak formulation

It is straightforward to obtain a weak formulation of the two-dimensional, electrostatic problem (2.7)–(2.8) for a fixed parameter z. Applying Stokes' theorem to the vector equation gives

$$\oint_C \boldsymbol{E}_{0,xy}(z,\boldsymbol{\xi}) \cdot d\boldsymbol{\xi} = 0 \tag{2.11}$$

for each closed, piecewise regular curve C in the plane. Applying the Gauss divergence theorem in two dimensions to the scalar equation results in

$$\begin{aligned} 0 &= \iint_\Omega \phi(x,y) \nabla_{xy} \cdot \boldsymbol{D}_{0,xy}(z,x,y)\, dx\, dy \\ &= -\iint_\Omega \boldsymbol{D}_{0,xy}(z,x,y) \cdot \nabla_{xy} \phi(x,y)\, dx\, dy \end{aligned} \tag{2.12}$$

for each two-dimensional, periodic test function

$$\phi(x,y) = \phi(x + mp_x, y + np_y)$$

To obtain (2.12) the periodicity of $\boldsymbol{D}_{0,xy}(z,\boldsymbol{\xi})$ has been used.

3 Numerical solution by FEM

In this section we analyze the two-dimensional static problem, (2.7)–(2.8) for a fixed parameter z, numerically using the finite element method (FEM). Specifically, we adopt the edge-element approach, and we recommend the papers by Bossavit as collateral reading on this subject [5–7]. Other relevant references are: [18, 21, 25, 27, 28]. The reader that is interested in the vast literature on FEM is recommended to consult the selected bibliography in Ref. 9 and the recent book [26].

3.1 Mesh and basis functions

Let n and m, respectively, be the number of nodes in the x- and y-directions of the chosen rectangular net of the unit cell, see Figure 2. Naturally, one can define nodes in the entire plane using the periodicity. Numerically, it is convenient to endow the unit cell with a "one-step" frame of nodes, which is well defined by periodicity. Such an extended unit cell is depicted in Figure 2. Furthermore, in concordance with standard FEM techniques, we triangularize the extended unit cell by introducing a diagonal in each rectangular mesh between the node in the lower left corner and the node in the upper right corner, see Figure 2.

Nodes are indicated by i, j, k, *etc.*. It is superfluous to refer specifically to nodes outside the extended unit cell and to nodes located at the right boundary or the upper boundary of the extended unit cell. Considering this, moving from the left to the right and row by row upwards, we number the remaining nodes of the extended

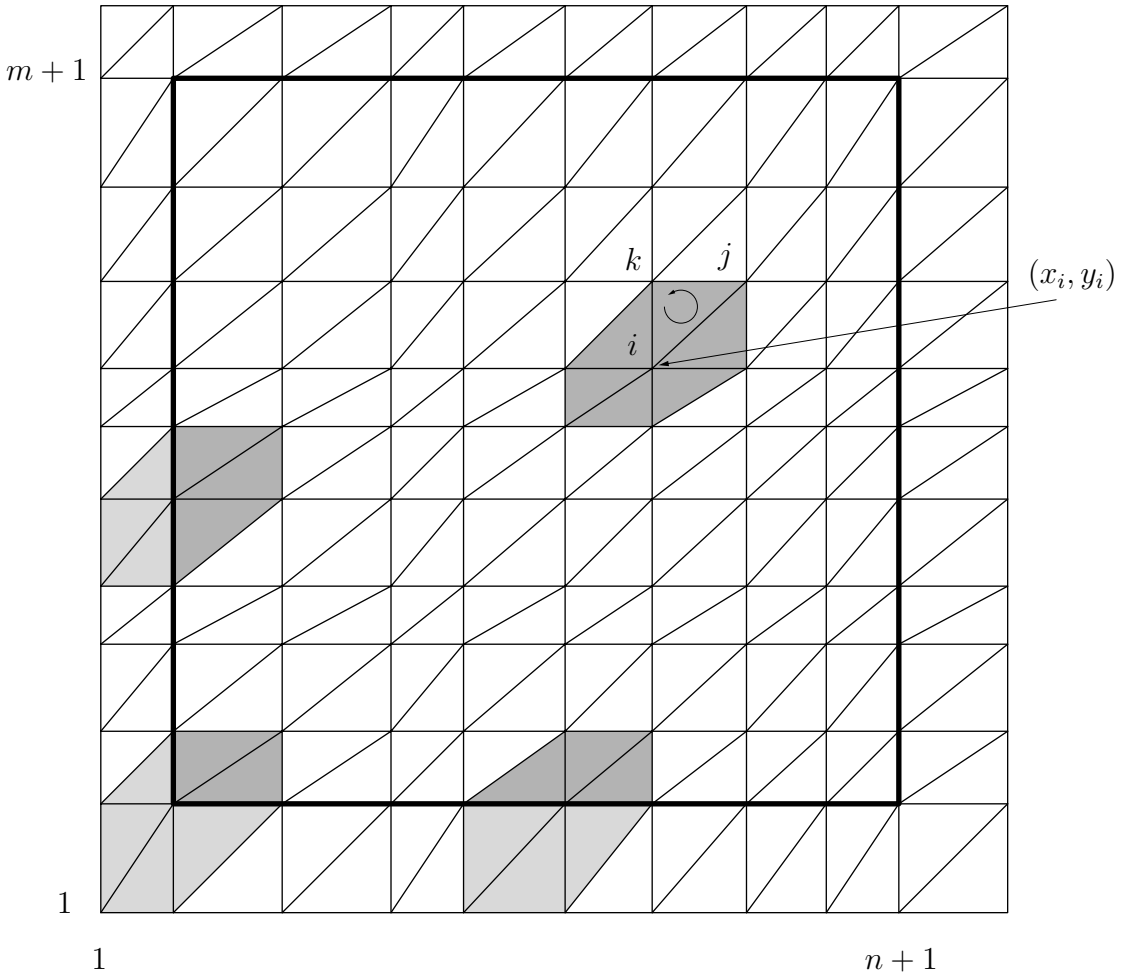

Figure 2: The mesh of the extended unit cell, the unit cell (heavy line), and the support of the functions $\lambda_i(x, y)$ centered at an interior point, at two edge points, and at a corner point of the unit cell. Areas with lighter shading represent the support of the function $\lambda_i(x, y)$ outside the unit cell.

unit cell by $1, 2, 3, \ldots, (n+1)(m+1)$. The set of numbered nodes is denoted by $\mathcal{N}$, and a node j in $\mathcal{N}$ is said to be adjacent a fixed node i in $\mathcal{N}$ if $j = i + 1$, $j = i + 1 + n$, or $j = i + 2 + n$. Formally, this definition does not apply to nodes located at the right boundary or the upper boundary of the unit cell; however, by referring to periodicity, three adjacent nodes can be defined analogously for any node in the plane. If node j is adjacent to node i (in the wide sense), we refer to the line segment between these nodes directed from i towards j as an "edge" and denote it by $\{i, j\}$.

Each node i is represented by its rectangular coordinates (x_i, y_i) and each node i in $\mathcal{N}$ is represented also by the ordered pair of integers (i_x, i_y), where $1 \le i_x \le n+1$ and $1 \le i_y \le m+1$. The one-to-one correspondence between the set $\mathcal{N}$ and the set of ordered pairs $\{(i_x, i_y),\ 1 \le i_x \le n+1,\ 1 \le i_y \le m+1\}$ is given by

$$i = (n+1)(i_y - 1) + i_x$$

The nodes that belong to the unit cell are: $2 \le i_x \le n+1$ and $2 \le i_y \le m+1$.

We also want to number the edges emanating from the numbered nodes $\mathcal{N}$. An appropriate one-to-one correspondence between the set of numbered edges $\mathcal{E}$ in the extended unit cell and the set of integers $\{1, 2, 3, \ldots, 3(n+1)(m+1)\}$ is

$$\begin{aligned}\{i, i+1\} &\leftrightarrow 3\left[(n+1)(i_y-1)+i_x-1\right]+1\\ \{i, i+2+n\} &\leftrightarrow 3\left[(n+1)(i_y-1)+i_x-1\right]+2\\ \{i, i+1+n\} &\leftrightarrow 3\left[(n+1)(i_y-1)+i_x-1\right]+3\end{aligned}$$

Here one should be philosophical about the left members in these expressions when $i_x = n+1$ or $i_y = m+1$.

About each node i, we define a "roof-top" or "tent" function. A general formulation of these node elements is presented in Appendix B, specifically Section B.1 and equation (B.4). The explicit expressions of the functions λ_i associated with node i that is appropriate in this paper can be found in Appendix C, see (C.1). The "tent" function λ_i is (or rather can be extended to) a continuous and piecewise linear function with compact support that is centered about node i. The largest value of λ_i is assumed at the center: $\lambda_i(x_i, y_i) = 1$. We wish to extend the "tent" functions periodically in both directions and denote the periodic extension of λ_i by $\widetilde{\lambda}_i$. The supports of some "tent" functions are indicated in Figure 2 using different grey tones to indicate whether the support is inside the unit cell or outside in the extended unit cell. The number of periodically extended "tent" functions is $(n-1)(m-1)$.

The vector basis function associated with the edge $\{i, j\}$ is defined by

$$\boldsymbol{\omega}_{\{i,j\}}(x, y) = \lambda_i(x, y)\nabla_{xy}\lambda_j(x, y) - \lambda_j(x, y)\nabla_{xy}\lambda_i(x, y)$$

A general formulation of these edge elements is presented in Appendix B, specifically Section B.2. The edge elements are piecewise linear (vector-valued) functions with compact support; specifically, $\boldsymbol{\omega}_{\{i,j\}}$ has support in the two mesh triangles that have the edge $\{i, j\}$ in common. One advantage with these particular basis functions is that their "tangential" components are continuous over the edges, see Appendix B; specifically, the tangential component of $\boldsymbol{\omega}_{\{i,j\}}$ along $\{i, j\}$ is the only non-zero component, and the orthogonality condition (B.7) holds. The explicit expressions for the edge elements adopted in this paper can be found in Appendix C.

3.2 Expansions and weak formulation

By choosing the periodically extended "tent" functions

$$\widetilde{\lambda}_k(x, y), \quad 2 \le k_x \le n,\ 2 \le k_y \le m$$

as test functions, the scalar equation (2.12) reduces to

$$0 = \iint_{\Omega} \boldsymbol{D}_{0,xy}(z, x, y) \cdot \nabla_{xy}\widetilde{\lambda}_k(x, y)\, dx\, dy \tag{3.1}$$

Hence the number of equations in (3.1) is $(n-1)(m-1)$.

The electric field can be written in the form

$$\boldsymbol{E}_{0,xy}(z,\boldsymbol{\xi}) = \sum_e \alpha_e(z)\boldsymbol{\omega}_e(\boldsymbol{\xi}) \tag{3.2}$$

where the index e runs over all edges in the entire plane ($\mathbb{R}^2$), and, owing to normalization (B.7), the coefficients are

$$\alpha_e(z) = \int_e \boldsymbol{E}_{0,xy}(z,\boldsymbol{\xi}) \cdot d\boldsymbol{l} \tag{3.3}$$

The periodicity and (3.3) show that there are at most $3(n-1)(m-1)$ different coefficients in (3.2), but this fact is not exploited at this point. For the field restricted to the unit cell it suffices to let the sum run over the set of numbered edges $\mathcal{E}$.

Substituting the constitutive relations $\boldsymbol{D}_{0,xy}(z,x,y) = \epsilon(x,y,z)\boldsymbol{E}_{0,xy}(z,x,y)$ and the field expansion (3.2) into the weak formulation (3.1) gives

$$\sum_{e\in\mathcal{E}} b_{e;k}(z)\alpha_e(z) = 0 \tag{3.4}$$

where

$$b_{e;k}(z) = \iint \epsilon(x,y,z)\boldsymbol{\omega}_e(x,y) \cdot \nabla_{xy}\lambda_k(x,y)\,dx\,dy \tag{3.5}$$

and the periodicity has been used for the case $k_x = 2$ or $k_y = 2$. For a fixed k, only 12 elements $b_{e;k}(z)$ are non-zero. Assuming that $\epsilon(x,y,z)$ is continuous within each triangular region of the net, these elements can be computed easily, see Appendix B, specifically Section B.3. The explicit expressions for the geometry used in this paper can be found in Appendix C. Since the number of elements in $\mathcal{E}$ is $3(n+1)(m+1)$, the system of equations (3.4) can be written in the form

$$\mathbf{B}(z) \cdot \boldsymbol{\alpha}(z) = \mathbf{0} \tag{3.6}$$

where the matrix $\mathbf{B}(z)$ is of type $(n-1)(m-1) \times 3(n+1)(m+1)$, and $\boldsymbol{\alpha}(z)$ is a vector, whose elements are $\alpha_e(z)$, $e \in \mathcal{E}$.

Up to now, we have not fully exploited the periodicity of the problem or the vector equation (zero circulation of $\boldsymbol{E}$) (2.11). Integrating the electric field along the mesh triangles shows that the coefficients $\alpha_e(z)$, $e \in \mathcal{E}$, are not independent; specifically,

$$\begin{cases} \alpha_{\{i,i+1\}}(z) + \alpha_{\{i+1,i+2+n\}}(z) - \alpha_{\{i,i+2+n\}}(z) = 0 \\ \alpha_{\{i,i+2+n\}}(z) - \alpha_{\{i+1+n,i+2+n\}}(z) - \alpha_{\{i,i+1+n\}}(z) = 0 \end{cases} \tag{3.7}$$

In addition, periodicity relates the coefficients $\alpha_e(z)$, $e \in \mathcal{E}$, to each other. The number of equations in the extended unit cell, see Figure 2, obtained this way is[4]

[4]In obtaining this number, we have already the tree structure in Section 3.3 in mind.

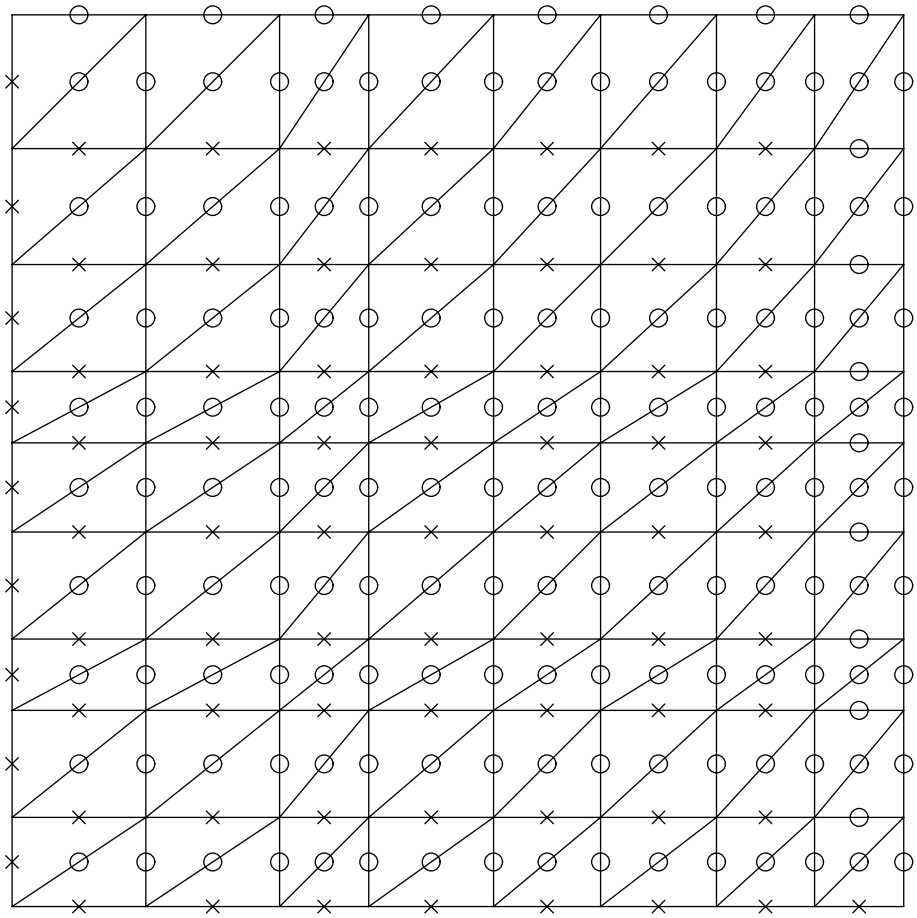

Figure 3: One representation of the "tree" structure in the unit cell where the "independent" edges are marked by $\times$ and the "dependent" edges by $\circ$.

$s = 6(n+m)+2(n-1)(m-1)-1 = 2nm+4(n+m)+1$; therefore, equations (3.7) can be written in the form

$$\mathbf{A} \cdot \boldsymbol{\alpha}(z) = \mathbf{0} \tag{3.8}$$

where $\mathbf{A}$ is a matrix of type $s \times 3(n+1)(m+1)$, which entries are either 0, 1, or -1.

3.3 Tree structure

We wish to obtain the two linearly independent solutions to problem (2.7)–(2.8) numerically, that is, two linearly independent solutions to the system of equations formed by (3.8) and (3.6). The first step is to introduce a "tree" structure in the unit cell and thereby define "independent" and "dependent" edges in $\mathcal{E}$. This can be done in a constructive way and an example of such a structure is presented in Figure 3, where the "independent" edges are marked by $\times$ and the "dependent" edges by $\circ$. Of course, the edges at the frame are all "dependent" due to periodicity. The "dependent" edges can be eliminated using (3.8). It is obvious that the "independent" edges are not uniquely defined. However, the number of "independent"

edges is always $(n-1)(m-1)+1$ and, consequently, the number of "dependent" edges is

$$6(n+m)+2(n-1)(m-1)-1 = 3(n+1)(m+1)-((n-1)(m-1)+1) = s$$

We denote the set of "independent" edges by $\mathcal{E}'$ and the set of "dependent" edges by $\mathcal{E}''$; thus, $\mathcal{E} = \mathcal{E}' \cup \mathcal{E}''$, and decompose the vector $\boldsymbol{\alpha}(z)$ belonging to these sets by the vectors $\boldsymbol{\alpha}'(z)$ and $\boldsymbol{\alpha}''(z)$, respectively. The curl equation (3.8) can now be written in the form

$$\mathbf{A}' \cdot \boldsymbol{\alpha}'(z) + \mathbf{A}'' \cdot \boldsymbol{\alpha}''(z) = \mathbf{0}$$

where $\mathbf{A}'$ is a matrix of type $s \times (n-1)(m-1)+1$ and $\mathbf{A}''$ is a quadratic matrix of type $s \times s$. Since introducing a "tree" structure is a constructive technique to express the elements in $\mathcal{E}''$ in terms of the elements in $\mathcal{E}'$, we can write

$$\boldsymbol{\alpha}''(z) = \mathbf{S} \cdot \boldsymbol{\alpha}'(z) \tag{3.9}$$

where the matrix $\mathbf{S}$ of type $s \times (n-1)(m-1)+1$ is given by

$$\mathbf{S} = -\left(\mathbf{A}''\right)^{-1} \cdot \mathbf{A}'$$

The entries of $\mathbf{S}$ are either 0, 1, or -1. Now equation (3.6) can be written as

$$\mathbf{B}'(z) \cdot \boldsymbol{\alpha}'(z) + \mathbf{B}''(z) \cdot \boldsymbol{\alpha}''(z) = \mathbf{0}$$

where $\mathbf{B}'$ is a matrix of type $(n-1)(m-1) \times (n-1)(m-1)+1$ and $\mathbf{B}''$ is a matrix of type $(n-1)(m-1) \times s$. Introducing (3.9) in this equation gives

$$\mathbf{M}(z) \cdot \boldsymbol{\alpha}'(z) = \mathbf{0} \tag{3.10}$$

where the matrix $\mathbf{M}$ of type $(n-1)(m-1) \times (n-1)(m-1)+1$ is

$$\mathbf{M}(z) = \mathbf{B}'(z) + \mathbf{B}''(z) \cdot \mathbf{S}$$

Nontrivial solutions, $\boldsymbol{\alpha}'(z)$, to the reduced problem belong to the null space of $\mathbf{M}$, which, by definition, is at least one-dimensional—the number of unknowns in (3.10) exceeds the number of equations by one. The null space is expected to be "numerically" two-dimensional, see the discussion of the periodic static problem below equation (2.8).

3.4 The solution (SVD)

The null space of $\mathbf{M}$ can be obtained by singular value decomposition (SVD), see Appendix A, in particular, equation (A.1). MATLAB supports numerical SVD. We expect precisely one singular value of $\mathbf{M}$ be much smaller than the others (approximately zero). This singular value defines one of the vectors that span the

"approximately" two-dimensional null space of $\mathbf{M}$, namely, $\boldsymbol{v}_{(n-1)(m-1)}$. The "approximate" null space is then spanned by $\boldsymbol{v}_{(n-1)(m-1)}$ and $\boldsymbol{v}_{(n-1)(m-1)+1}$, see (A.1). To this end, the two linearly independent solutions to (3.10) are

$$\begin{cases} \boldsymbol{\alpha}_1'(z) = \boldsymbol{v}_{(n-1)(m-1)+1} \\ \boldsymbol{\alpha}_2'(z) = \boldsymbol{v}_{(n-1)(m-1)} \end{cases}$$

Once the two "independent" solutions, $\boldsymbol{\alpha}_1'(z)$ and $\boldsymbol{\alpha}_2'(z)$, have been obtained, equation (3.9) gives the corresponding "dependent" solutions, $\boldsymbol{\alpha}_1''(z)$ and $\boldsymbol{\alpha}_2''(z)$. Therefore, two linearly independent solutions, (3.2), to the periodic problem (2.7)–(2.8) in a weak sense are

$$\begin{cases} \boldsymbol{E}_{0,xy,1}(z,\boldsymbol{\xi}) = \displaystyle\sum_e \alpha_{e,1}(z)\boldsymbol{\omega}_e(\boldsymbol{\xi}) \\ \boldsymbol{E}_{0,xy,2}(z,\boldsymbol{\xi}) = \displaystyle\sum_e \alpha_{e,2}(z)\boldsymbol{\omega}_e(\boldsymbol{\xi}) \end{cases}$$

The effective permittivity dyadic is obtained from (2.9), where, due to periodicity

$$\begin{cases} <\boldsymbol{E}_{0,xy,p}(z,\boldsymbol{\xi})> = \displaystyle\sum_e \alpha_{e,p}(z) <\boldsymbol{\omega}_e(\boldsymbol{\xi})> \\ <\boldsymbol{D}_{0,xy,p}(z,\boldsymbol{\xi})> = \displaystyle\sum_e \alpha_{e,p}(z) <\epsilon(z,\boldsymbol{\xi})\boldsymbol{\omega}_e(\boldsymbol{\xi})> \end{cases} \qquad p = 1,2$$

and the index e runs over all edges that emanate from the nodes i corresponding to $2 \le i_x \le n$, $2 \le i_y \le m$.

The average values $<\epsilon(z,\boldsymbol{\xi})\boldsymbol{\omega}_e(\boldsymbol{\xi})>$ are easy to obtain using the mean value theorem of integral calculus (we assume the permittivity to be continuous within each triangular region), see Appendix B, specifically Section B.3. Explicit expressions relevant for the geometry used in this paper can be found in Appendix C.

4 Numerical results

In Figure 4, the numerical result for the effective permittivity components of a two-phase medium that is layered in the x-direction is presented. The relative permittivities of the constituents are $\epsilon_1 = 1$ and $\epsilon_2 = 2$. The numerical result agrees excellently with the theoretical result (2.10) already for $m = 2$ and $n = 11$.

For a periodic square $(p \times p)$ array of square rods of cross-section $a \times a$ and relative permittivity ϵ_2, embedded in a host matrix of permittivity ϵ_1, one has

$$\boldsymbol{\epsilon}_{\text{eff}}/\epsilon_0 = (\hat{\boldsymbol{x}}\hat{\boldsymbol{x}} + \hat{\boldsymbol{y}}\hat{\boldsymbol{y}})\,\epsilon_{\text{eff},\perp\perp} + \hat{\boldsymbol{z}}\hat{\boldsymbol{z}}\epsilon_{\text{eff},zz}, \tag{4.1}$$

where $\epsilon_{\text{eff},zz} = \epsilon_1 + (\epsilon_2 - \epsilon_1)g$ and $g = a^2/p^2$ for the case the rods are extended in the z-direction. An approximate solution for the effective parameter $\epsilon_{\text{eff},\perp\perp}$ is given by the Hashin-Shtrikman formula, see, *e.g.*, [16]:

$$\epsilon_{\text{eff},\perp\perp} = \epsilon_1 \left(1 + 2g\frac{\epsilon_2 - \epsilon_1}{(1+g)\epsilon_1 + (1-g)\epsilon_2}\right) \tag{4.2}$$

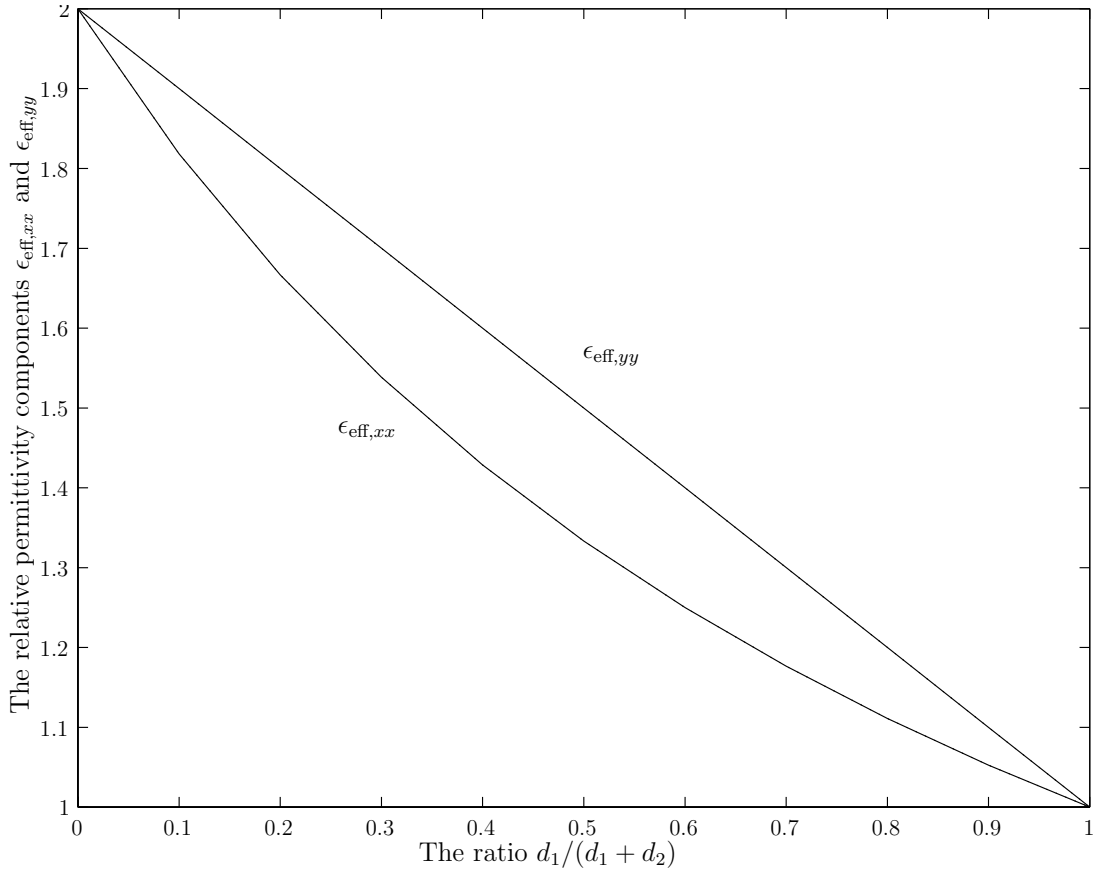

Figure 4: Numerical results for the effective permittivity components of a two-phase medium that is layered in the x-direction.

In Figure 5, the numerical result ($m = n = 11$) for $\epsilon_{\text{eff},\perp\perp}$ is compared to the Hashin-Shtrikman formula for an array characterized by $\epsilon_1 = 1$ and $\epsilon_2 = 10$.

Finally, we consider the simple woven composite material in Figure 6. Due to symmetry it is sufficient to consider a quarter of the unit cell only and this approach is customary in the literature. However, in order not to loose generality, this fact has not been exploited in this article.

For simplicity, we assume that the warp and fill yarns are identical with permittivity ϵ_2. The permittivity of the host matrix is denoted by ϵ_1. The explicit values of the permittivity are given in Table 1. The effective permittivity can be written in the form (4.1), that is, the medium is effectively uniaxial. Due to symmetry, $\boldsymbol{\epsilon}_{\text{eff}}(z) = \boldsymbol{\epsilon}_{\text{eff}}(|z|)$, where the extent of the weave in the normal direction is defined by $|z| < h$. The height and the width of the warp and fill yarns are denoted by h and a, respectively, and the width of the gap between neighboring yarns is g, see Figure 6. The period is then $p = 2(a + g)$ in both the transverse directions. The weave is symmetrically embedded in the host matrix and the total thickness of the structure in Figure 6 is $2(h + d)$. The volume fraction of yarn is $v_f = 1/(1 + r)(1 + q)$, where $q = g/a$ and $r = d/h$.

Numerical results ($m = n = 25$) for the real and imaginary parts of the effective

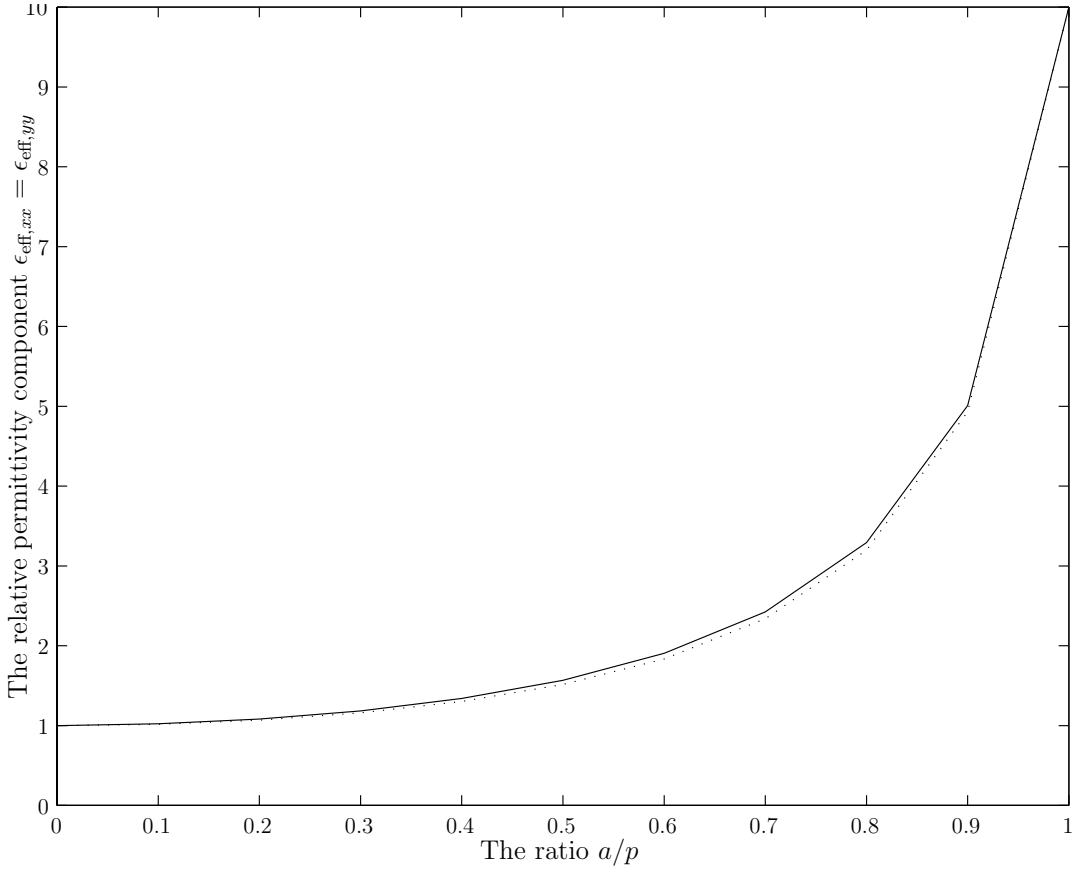

Figure 5: Numerical results for a periodic array of square rods. The dotted curve represents the Hashin-Shtrikman formula, see (4.2).

parameter $\epsilon_{\text{eff},\perp\perp}(z)$ of three different panels are presented in Figures 7–8, respectively. In all three cases, the width of the yarn is $a = 5h$. In Figures 7–8, the mean tilt angle of the warp and fill yarns is varied under constant volume fraction of yarn $v_f = 0.2667$. This is reflected in different values of the ratios q and r. The effective parameter $\epsilon_{\text{eff},zz}(z)$ is found to be, see (2.6)

$$\epsilon_{\text{eff},zz}(z) = \begin{cases} \epsilon_1 + (\epsilon_2 - \epsilon_1)4a\left(a + 2g(1 - |z|/h)\right)/p^2, & |z| < h \\ \epsilon_1, \qquad h < |z| < h + d \end{cases}$$

The real and imaginary parts of this component are plotted in Figures 7–8 also.

5 Dynamics of the average field—homogenization

In previous sections we obtained the effective permittivity and permeability dyadics of a two-periodic composite medium. In general, these dyadics depend on the normal coordinate z. In this section, we discuss the resulting ordinary differential equations, (2.3), for the average fields. In particular, we focus on the reflection and transmission properties of a thin stratified uniaxial layer with its optical axis in the normal direction.

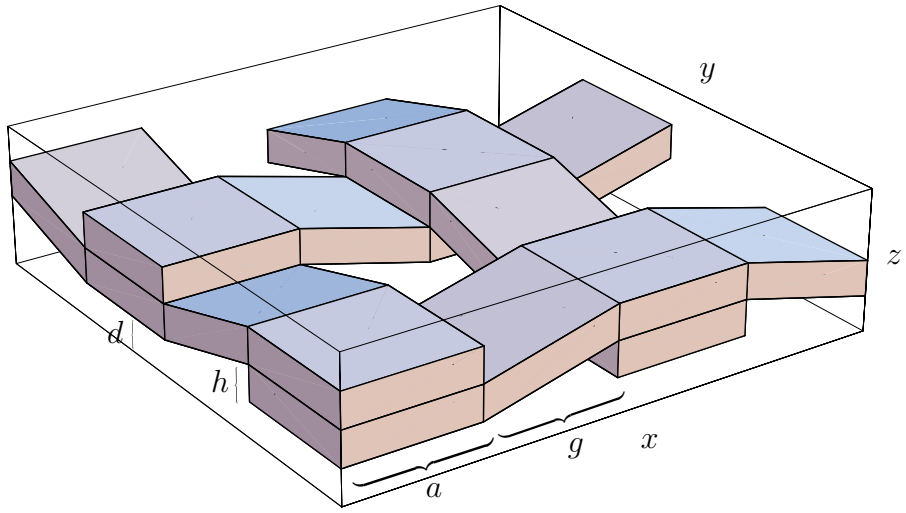

Figure 6: A simple model of a woven composite material.

	ϵ
ϵ_1 (Epoxy)	$3.65(1 + i0.0320)$
ϵ_2 (E-glass)	$6.32(1 + i0.0037)$

Table 1: The permittivity of the host material, ϵ_1, and the permittivity of the warp and fill yarns, ϵ_2.

5.1 Plane wave expansion

In a geometry where the medium is laterally homogeneous in the variables x and y, it is natural to decompose the electromagnetic field in a spectrum of plane waves [8]. The plane wave decomposition amounts to Fourier transformation of the electric and magnetic fields and flux densities with respect to the lateral variables x and y. The Fourier transform of a time-harmonic field $\boldsymbol{E}(\boldsymbol{r}, \omega)$ is denoted by

$$\boldsymbol{E}(z, \boldsymbol{k}_t, \omega) = \iint_{-\infty}^{\infty} \boldsymbol{E}(\boldsymbol{r}, \omega) e^{-i\boldsymbol{k}_t \cdot \boldsymbol{\rho}} \, dxdy$$

where

$$\boldsymbol{k}_t = \hat{\boldsymbol{x}} k_x + \hat{\boldsymbol{y}} k_y = k_t \hat{\boldsymbol{e}}_{\parallel}$$

is the tangential wave vector and

$$k_t = \sqrt{k_x^2 + k_y^2}$$

the tangential wave number. We denote the position vector in the x-y-plane by $\boldsymbol{\rho} = \hat{\boldsymbol{x}} x + \hat{\boldsymbol{y}} y$.

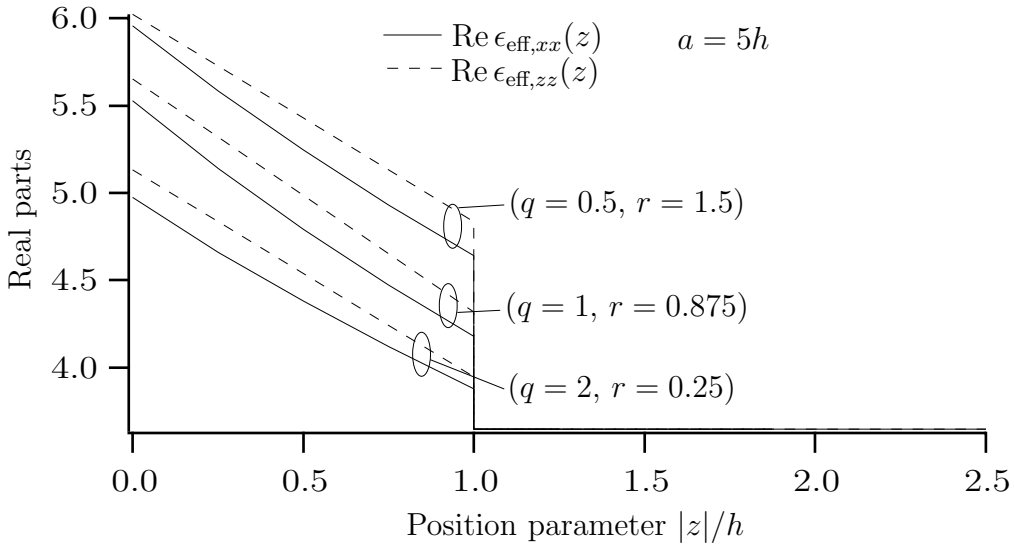

Figure 7: Real parts of the effective permittivity components of three different weaves.

The inverse Fourier transform is defined by

$$\boldsymbol{E}(\boldsymbol{r},\omega) = \frac{1}{4\pi^2}\iint_{-\infty}^{\infty} \boldsymbol{E}(z,\boldsymbol{k}_t,\omega)e^{i\boldsymbol{k}_t\cdot\boldsymbol{\rho}}\,dk_x dk_y$$

Notice that the same letter is used to denote the Fourier transform of the field and the field itself. The argument of the field shows what field is intended.

Below, the tangential wave vector, $\boldsymbol{k}_t$, is fixed but arbitrary. In a region where the material is laterally homogeneous, the Fourier transformed field (plane wave amplitude) satisfies a system of linear, coupled ordinary differential equations (ODEs)—the fundamental equation [22].

$$\frac{d}{dz}\begin{pmatrix}\boldsymbol{E}_{xy}(z,\boldsymbol{k}_t,\omega)\\ \eta_0\mathbf{J}\cdot\boldsymbol{H}_{xy}(z,\boldsymbol{k}_t,\omega)\end{pmatrix} = ik_0\mathbf{M}(z,\boldsymbol{k}_t,\omega)\cdot\begin{pmatrix}\boldsymbol{E}_{xy}(z,\boldsymbol{k}_t,\omega)\\ \eta_0\mathbf{J}\cdot\boldsymbol{H}_{xy}(z,\boldsymbol{k}_t,\omega)\end{pmatrix} \tag{5.1}$$

where $k_0 = \omega/c_0$ is the wave number in vacuum, $\mathbf{J} = \hat{\boldsymbol{z}}\times\mathbf{I}_2$ is a two-dimensional rotation dyadic (rotation of $\pi/2$ in the x-y-plane), $\mathbf{I}_2$ is the identity dyadic in the x-y-plane, and $\boldsymbol{E}_{xy}$ and $\boldsymbol{H}_{xy}$ are the transverse parts of the electric and the magnetic fields, respectively.

In vacuum regions, the solutions are either homogeneous, obliquely propagating plane waves or inhomogeneous plane waves depending on whether the tangential wave number, k_t, is less or greater than the wave number in vacuum, k_0. It is appropriate to introduce an angle of incidence, θ_i, which is real for homogeneous plane waves, and a normal wave number, k_z, defined by

$$k_z = k_0\cos\theta_i = \left(k_0^2 - k_t^2\right)^{1/2} = \begin{cases}\sqrt{k_0^2 - k_t^2} \text{ for } k_t < k_0\\ i\sqrt{k_t^2 - k_0^2} \text{ for } k_t > k_0\end{cases}$$

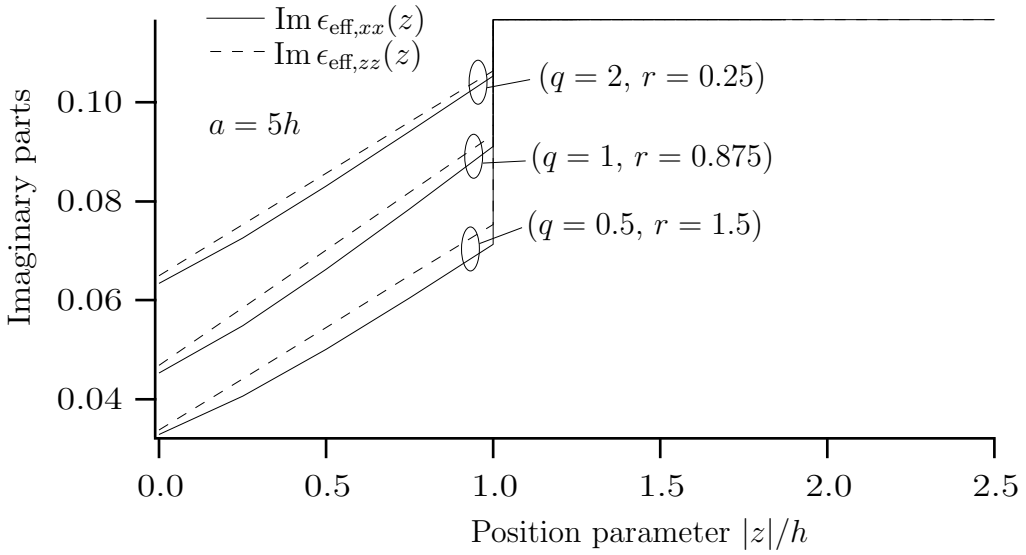

Figure 8: Imaginary parts of the effective permittivity components of three different weaves.

By this definition, k_z applies to the up-going wave and $-k_z$ to the down-going wave. Furthermore, it is convenient to introduce coordinate independent orthonormal basis vectors in the x-y plane by

$$\begin{cases} \hat{\boldsymbol{e}}_{\parallel} = \boldsymbol{k}_t / k_t \\ \hat{\boldsymbol{e}}_{\perp} = \hat{\boldsymbol{z}} \times \hat{\boldsymbol{e}}_{\parallel} \end{cases}$$

The basis vectors $\hat{\boldsymbol{e}}_{\parallel}$, $\hat{\boldsymbol{e}}_{\perp}$, $\hat{\boldsymbol{z}}$ form a positively oriented ON-system.

The solution of the fundamental equation, (5.1), formally defines the propagator of the fields, $\mathbf{P}(z_2, z_1, \boldsymbol{k}_t, \omega)$, which takes the tangential field from position z_1 to position z_2 [22], *i.e.*,

$$\begin{pmatrix} \boldsymbol{E}_{xy}(z_2, \boldsymbol{k}_t, \omega) \\ \eta_0 \mathbf{J} \cdot \boldsymbol{H}_{xy}(z_2, \boldsymbol{k}_t, \omega) \end{pmatrix} = \mathbf{P}(z_2, z_1, \boldsymbol{k}_t, \omega) \cdot \begin{pmatrix} \boldsymbol{E}_{xy}(z_1, \boldsymbol{k}_t, \omega) \\ \eta_0 \mathbf{J} \cdot \boldsymbol{H}_{xy}(z_1, \boldsymbol{k}_t, \omega) \end{pmatrix}$$

This concept of propagators is thoroughly analyzed in Ref. [22].

5.2 Homogenization of a thin uniaxial layer

The propagator at oblique incidence for a thin uniaxial medium ($z_1 < z < z_2$), which is laterally homogeneous, is approximately given by [22]

$$\begin{aligned} \begin{pmatrix} \boldsymbol{E}_{xy}(z_2) \\ \eta_0 \mathbf{J} \cdot \boldsymbol{H}_{xy}(z_2) \end{pmatrix} =& \mathbf{P}(z_2, z_1) \cdot \begin{pmatrix} \boldsymbol{E}_{xy}(z_1) \\ \eta_0 \mathbf{J} \cdot \boldsymbol{H}_{xy}(z_1) \end{pmatrix} \\ \approx& \exp\left\{ ik_0 \int_{z_1}^{z_2} \mathbf{M}(z)\, dz \right\} \cdot \begin{pmatrix} \boldsymbol{E}_{xy}(z_1) \\ \eta_0 \mathbf{J} \cdot \boldsymbol{H}_{xy}(z_1) \end{pmatrix} \end{aligned}$$

	$\epsilon_{\text{eff},\perp\perp}$	$\epsilon_{\text{eff},zz}$
$q = 2.0,\ r = 0.250$	$4.2482 + i.0902$	$4.3102 + i.0967$
$q = 1.0,\ r = 0.875$	$4.2709 + i.0902$	$4.2468 + i.1022$
$q = 0.5,\ r = 1.500$	$4.2961 + i.0904$	$4.1961 + i.1061$

Table 2: The effective permittivity components of a thin weave. The yarn volume fraction is $v_f = 1/(1+r)(1+q) = 0.2667$ in all three cases.

where the fundamental dyadic [22] is

$$\mathbf{M}(z) = \begin{pmatrix} \mathbf{0} & -\mathbf{I}_2 + \frac{1}{\epsilon_{zz}(z)k_0^2}\boldsymbol{k}_t\boldsymbol{k}_t \\ -\epsilon_{\perp\perp}(z)\mathbf{I}_2 - \frac{1}{k_0^2}\mathbf{J}\cdot\boldsymbol{k}_t\boldsymbol{k}_t\cdot\mathbf{J} & \mathbf{0} \end{pmatrix}$$

and $\boldsymbol{k}_t$ is the tangential wave vector. The effective permittivity components for the uniaxial slab are therefore

$$\begin{cases} (z_1 - z_2)\epsilon_{\text{eff},\perp\perp} = \displaystyle\int_{z_1}^{z_2} \epsilon_{\perp\perp}(z)\,dz \\ \dfrac{z_1 - z_2}{\epsilon_{\text{eff},zz}} = \displaystyle\int_{z_1}^{z_2} \frac{1}{\epsilon_{zz}(z)}\,dz \end{cases}$$

For the weave in Section 4, the effective permittivity components are found to be

$$\begin{cases} \epsilon_{\text{eff},\perp\perp} = \dfrac{1}{1+r}\left(r\epsilon_1 + \dfrac{1}{h}\displaystyle\int_0^h \epsilon_{\perp\perp}(z)\,dz\right) \\ \epsilon_{\text{eff},zz} = \dfrac{1+r}{\frac{r}{\epsilon_1} + \frac{(1+q)^2}{2q(\epsilon_2-\epsilon_1)}\log\left(\frac{\epsilon_1+(\epsilon_2-\epsilon_1)(1+2q)/(1+q)^2}{\epsilon_1+(\epsilon_2-\epsilon_1)/(1+q)^2}\right)} \end{cases}$$

where, as above, $r = d/h$ and $q = g/a$.

In Table 2, the effective permittivity components are presented for three different choices of the parameters q and r but for the same volume fraction of yarn $v_f = 0.2667$. The results indicate that the effective medium parameters are relatively insensitive to variations of the mean tilt angle of the warp and fill yarns as long as the volume fraction of the yarn is held constant. These results can be compared to a result given by Agarwal and Dasgupta (for a weave of oval cross-section but of the same volume fraction yarn) using another method [1]: $\epsilon_{\text{eff},\perp\perp} = 4.29 + i.0987$ and $\epsilon_{\text{eff},zz} = 4.19 + i.1089$. Notice that for $q = 2$ the real part of $\epsilon_{\text{eff},\perp\perp}$ is less than the real part of $\epsilon_{\text{eff},zz}$ and that for $q = 1$ and $q = 0.5$ the real part of $\epsilon_{\text{eff},\perp\perp}$ is larger than the real part of $\epsilon_{\text{eff},zz}$. Notice also that the imaginary part of $\epsilon_{\text{eff},\perp\perp}$ is less than the imaginary part of $\epsilon_{\text{eff},zz}$ for all three values of q.

5.3 Reflection and transmission

The reflection dyadic for the tangential electric field at oblique incidence of a homogeneous uniaxial layer with its optical axis in the z-direction (thickness d, per-

mittivity values $\epsilon_{\perp\perp}$ and ϵ_{zz}) and which is located in vacuum can be written in the form [22]

$$\begin{cases} \mathbf{r} = \hat{\boldsymbol{e}}_{\parallel}\hat{\boldsymbol{e}}_{\parallel} r_{\parallel\parallel} + \hat{\boldsymbol{e}}_{\perp}\hat{\boldsymbol{e}}_{\perp} r_{\perp\perp} \\ \mathbf{t} = \hat{\boldsymbol{e}}_{\parallel}\hat{\boldsymbol{e}}_{\parallel} t_{\parallel\parallel} + \hat{\boldsymbol{e}}_{\perp}\hat{\boldsymbol{e}}_{\perp} t_{\perp\perp} \end{cases}$$

where

$$\begin{cases} r_{\parallel\parallel} = r_{1\parallel\parallel} \dfrac{1 - e^{2ik_0\lambda_- d}}{1 - r_{1\parallel\parallel}^2 e^{2ik_0\lambda_- d}} \\ r_{\perp\perp} = r_{1\perp\perp} \dfrac{1 - e^{2ik_0\lambda_+ d}}{1 - r_{1\perp\perp}^2 e^{2ik_0\lambda_+ d}} \end{cases} \qquad \begin{cases} t_{\parallel\parallel} = \dfrac{(1 - r_{1\parallel\parallel}^2) e^{ik_0\lambda_- d}}{1 - r_{1\parallel\parallel}^2 e^{2ik_0\lambda_- d}} \\ t_{\perp\perp} = \dfrac{(1 - r_{1\perp\perp}^2) e^{ik_0\lambda_+ d}}{1 - r_{1\perp\perp}^2 e^{2ik_0\lambda_+ d}} \end{cases}$$

Here the Fresnel equations are

$$\begin{cases} r_{1\parallel\parallel} = \dfrac{\lambda_- - \epsilon_{\perp\perp}\cos\theta_i}{\lambda_- + \epsilon_{\perp\perp}\cos\theta_i} \\ r_{1\perp\perp} = \dfrac{\cos\theta_i - \lambda_+}{\cos\theta_i + \lambda_+} \end{cases}$$

where the eigenvalues of the fundamental dyadic are

$$\lambda_+^2 = \epsilon_{\perp\perp} - \frac{k_t^2}{k_0^2}, \qquad \lambda_-^2 = \epsilon_{\perp\perp} - \frac{k_t^2}{k_0^2}\frac{\epsilon_{\perp\perp}}{\epsilon_{zz}}$$

6 Conclusions

In this paper, we present a homogenization scheme for a complex two-component mixture, *e.g.*, woven materials. The analysis exploits the multiple-scale technique, and the numerical solution of the two-dimensional vector-valued problem is found by a FEM formulation, which, due to the periodic boundary conditions of the problem, is non-standard. Basically, the static problem is solved on a torus and there are exactly two independent solution of this problem which are used in the solution of the homogenization problem. The reflection and transmission properties of the homogenized material are also investigated.

Acknowledgment

The authors would like to thank Professor Erkki Somersalo at Helsinki University of Technology for most useful advice concerning this article. The work reported in this paper is supported by a grant from the Defence Materiel Administration of Sweden (FMV) and its support is gratefully acknowledged.

Appendix A Singular value decomposition

Singular value decomposition (SVD) is an important and well known technique in modern numerical linear algebra to factor a general complex-valued matrix. In this appendix, we repeat basic results of SVD that are relevant to us.

Recall that a complex-valued matrix $\mathbf{V}$ of type $n \times n$ is said to be unitary if $\mathbf{V}\mathbf{V}^H = \mathbf{I}_n$, where $\mathbf{V}^H$ denotes the Hermite transpose (conjugate transpose) of $\mathbf{V}$ and $\mathbf{I}_n$ is the identity matrix (of type $n \times n$). Moreover, $\mathbf{V}$ is said to be Hermitian if $\mathbf{V} = \mathbf{V}^H$. The spectral theorem applies to Hermitian matrices.

Theorem A.1. *Let r be the rank of the complex-valued $m \times n$-matrix $\mathbf{M}$. Then there is*

1. *a sequence of unique real numbers, $\{\sigma_i\}_{i=1}^r$, $\sigma_1 \geq \sigma_2 \geq \ldots \geq \sigma_r > 0$*
2. *a unitary $m \times m$-matrix $\mathbf{U} = \begin{pmatrix} \boldsymbol{u}_1 & \boldsymbol{u}_2 & \ldots & \boldsymbol{u}_m \end{pmatrix}$*
3. *a unitary $n \times n$-matrix $\mathbf{V} = \begin{pmatrix} \boldsymbol{v}_1 & \boldsymbol{v}_2 & \ldots & \boldsymbol{v}_n \end{pmatrix}$*
4. *and a $m \times n$-matrix $\boldsymbol{\Sigma} = \begin{pmatrix} \mathbf{D}_r & \mathbf{0} \\ \mathbf{0} & \mathbf{0} \end{pmatrix}$ where $\mathbf{D}_r = \operatorname{diag}(\sigma_1, \sigma_2, \ldots, \sigma_r)$*

such that $\mathbf{M}$ can be factored as

$$\mathbf{M} = \mathbf{U}\boldsymbol{\Sigma}\mathbf{V}^H = \sigma_1 \boldsymbol{u}_1 \boldsymbol{v}_1^H + \ldots + \sigma_r \boldsymbol{u}_r \boldsymbol{v}_r^H$$

The vectors $\boldsymbol{u}_i$ in the notation $\begin{pmatrix} \boldsymbol{u}_1 & \boldsymbol{u}_2 & \ldots & \boldsymbol{u}_m \end{pmatrix}$ are interpreted as column vectors.

The positive real numbers, $\{\sigma_i\}_{i=1}^r$, are referred to as the positive singular values of $\mathbf{M}$. The vectors $\boldsymbol{u}_i$, $1 \leq i \leq r$ are eigenvectors of the non-negative definite and Hermitian $m \times m$-matrix $\mathbf{M}\mathbf{M}^H$ with the eigenvalues σ_i^2, respectively, and the vectors $\boldsymbol{v}_i$, $1 \leq i \leq r$ are eigenvectors of the non-negative definite and Hermitian $n \times n$-matrix $\mathbf{M}^H\mathbf{M}$ with the eigenvalues σ_i^2, respectively. In addition,

$$\begin{cases} \boldsymbol{u}_i = \dfrac{1}{\sigma_i}\mathbf{M}\boldsymbol{v}_i, & 1 \leq i \leq r \\ \boldsymbol{v}_i = \dfrac{1}{\sigma_i}\mathbf{M}^H\boldsymbol{u}_i, & 1 \leq i \leq r \end{cases}$$

Clearly, the ranges of $\mathbf{M}$ and $\mathbf{M}\mathbf{M}^H$ coincide:

$$\operatorname{Im}(\mathbf{M}) = \operatorname{Im}\left(\mathbf{M}\mathbf{M}^H\right) = \operatorname{span}\{\boldsymbol{u}_1, \ldots, \boldsymbol{u}_r\}$$

The vectors $\boldsymbol{u}_i$, $r+1 \leq i \leq m$ are eigenvectors of $\mathbf{M}\mathbf{M}^H$ with the eigenvalues 0 and the vectors $\boldsymbol{v}_i$, $r+1 \leq i \leq n$ are eigenvectors of $\mathbf{M}^H\mathbf{M}$ with the eigenvalues 0. Above we refer to the fact that the null spaces of $\mathbf{M}$ and $\mathbf{M}^H\mathbf{M}$ coincide:

$$\operatorname{Ker}(\mathbf{M}) = \operatorname{Ker}\left(\mathbf{M}^H\mathbf{M}\right) = \operatorname{span}\{\boldsymbol{v}_{r+1}, \ldots, \boldsymbol{v}_n\} \tag{A.1}$$

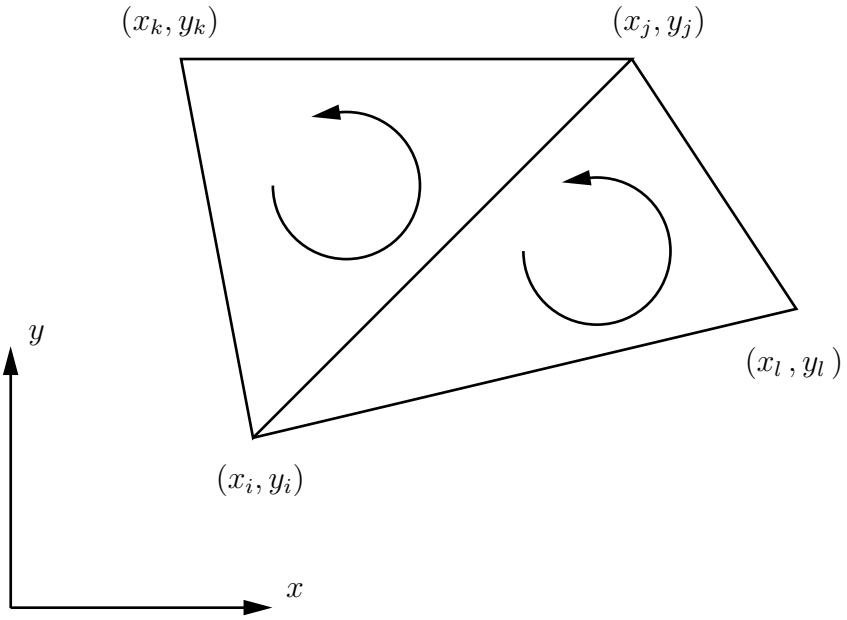

Figure 9: Definition of the triangle.

Appendix B Whitney fields

Using the terminology of the three-dimensional problem, the node elements (scalar basis functions) used in this paper are so-called Whitney fields of degree 0 and the edge elements (vector basis functions) are Whitney fields of degree 1 [5]. More on differential forms and the concept of simplices can be found in Flanders [13]. In this section we present some of the basic properties of these elements.

B.1 Node elements

Let the distinct, not collinear, points $i = (x_i, y_i)$, $j = (x_j, y_j)$, and $k = (x_k, y_k)$ in the x-y-plane be oriented in a right-hand sense, see Figure 9, and let these points define the vertices of a closed triangle T_{ijk}. Define constants a_{jk}, b_{jk}, and c_{jk} as

$$\begin{cases} a_{jk} = x_j y_k - x_k y_j \\ b_{jk} = y_j - y_k \\ c_{jk} = x_k - x_j \end{cases}$$

and denote the area of the triangle T_{ijk} by Δ_{ijk}:

$$2\Delta_{ijk} = \begin{vmatrix} 1 & x_i & y_i \\ 1 & x_j & y_j \\ 1 & x_k & y_k \end{vmatrix} = (x_j y_k - x_k y_j) + (x_k y_i - x_i y_k) + (x_i y_j - x_j y_i)$$

The piecewise linear function

$$\phi_{ijk}(x, y) = \begin{cases} \dfrac{a_{jk} + b_{jk} x + c_{jk} y}{2\Delta_{ijk}}, & (x, y) \in T_{ijk} \\ 0, \quad \text{otherwise} \end{cases}$$

then satisfies

$$\phi_{ijk}(x_p, y_p) = \delta_{ip}, \quad p = i, j, k$$

Moreover, ϕ_{ijk} is nonnegative

$$\phi_{ijk}(x, y) \geq 0 \text{ for all } (x, y) \tag{B.1}$$

and integrable with integral

$$\iint \phi_{ijk}(x, y)\, dxdy = \Delta_{ijk}/3 \tag{B.2}$$

For any real, scalar, and integrable function $\epsilon(x, y)$, which is continuous in T_{ijk}, the mean value theorem for multiple integrals [2, p. 269] gives

$$\iint \epsilon(x, y)\phi_{ijk}(x, y)\, dxdy = \epsilon(x_0, y_0)\Delta_{ijk}/3 \tag{B.3}$$

for some point $(x_0, y_0) \in T_{ijk}$, where the properties (B.1)–(B.2) have been used. Similarly, for each complex, scalar, and integrable function $\epsilon \equiv \epsilon' + i\epsilon''$ being continuous in T_{ijk}, where ϵ' is the real part of ϵ and ϵ'' is the imaginary part of ϵ, one gets

$$\iint \epsilon(x, y)\phi_{ijk}(x, y)\, dxdy = (\epsilon'(x_a, y_a) + i\epsilon''(x_b, y_b))\, \Delta_{ijk}/3$$

for some points (x_a, y_a) and (x_b, y_b) belonging to T_{ijk}.

For the quantities defined in the preceding paragraph the vertex i holds a unique position. By cyclic permutation, the corresponding quantities are defined for the vertices j and k. It is easy to verify that

$$\begin{cases} a_{jk} + a_{ki} + a_{ij} = 2\Delta_{ijk} \\ b_{jk} + b_{ki} + b_{ij} = 0 \\ c_{jk} + c_{ki} + c_{ij} = 0 \end{cases}$$

The continuous "tent-functions" referred to in the present paper consist of six piecewise linear basis functions of the type ϕ_{ijk}. More generally,

$$\lambda_i(x, y) = \sum_{m,n} \phi_{imn}(x, y) \tag{B.4}$$

where the nodes i, m, and n are oriented in the right-hand sense. Note that $\lambda_i(x_i, y_i) = 1$.

B.2 Edge elements

The edge elements can be expressed in terms of the node elements and gradients of the node elements. Specifically, the element associated with the edge $\{i,j\}$ (which is directed from i to j) is the piecewise linear vector field

$$\boldsymbol{\omega}_{\{i,j\}}(x,y) = \lambda_i(x,y)\nabla_{xy}\lambda_j(x,y) - \lambda_j(x,y)\nabla_{xy}\lambda_i(x,y)$$

which can be written as

$$\begin{aligned}\boldsymbol{\omega}_{\{i,j\}}(x,y) = \phi_{ijk}(x,y)\frac{(b_{ki},c_{ki})}{2\Delta_{ijk}} - \phi_{jki}(x,y)\frac{(b_{jk},c_{jk})}{2\Delta_{ijk}} \\ + \phi_{ilj}(x,y)\frac{(b_{il},c_{il})}{2\Delta_{ilj}} - \phi_{jil}(x,y)\frac{(b_{lj},c_{lj})}{2\Delta_{ilj}}\end{aligned} \tag{B.5}$$

where $i = (x_i, y_i)$, $j = (x_j, y_j)$, $k = (x_k, y_k)$, and $l = (x_l, y_l)$ are distinct points in the x-y-plane that are oriented in the right-hand sense, see Figure 9, and (b_{ki}, c_{ki}) denotes the point in the x-y-plane at which $x = b_{ki}$ and $y = c_{ki}$ *etc.*. The two first terms in the right member of (B.5) have support in the triangle T_{ijk}, whereas the two last terms have support in the triangle T_{ilj}; thus, $\boldsymbol{\omega}_{\{i,j\}}$ has support in those triangles that have the edge $\{i,j\}$ in common. Clearly, the vector basis function $\boldsymbol{\omega}_{\{i,j\}}$ depends on the points k and l, but to avoid a cumbersome notation these indices are not explicitly written out. Notice that the edge $\{i,j\}$ is different from $\{j,i\}$ and that only one of these edges belongs to the set of edges defined by the net. The relation between the edge element associated with $\{j,i\}$ and the one associated with $\{i,j\}$ is

$$\boldsymbol{\omega}_{\{j,i\}}(x,y) = -\boldsymbol{\omega}_{\{i,j\}}(x,y) \tag{B.6}$$

One of the more salient features of the edge element $\boldsymbol{\omega}_{\{i,j\}}$ is that its tangential component vanishes identically on the boundary of its support, that is, along the edges $\{j,k\}$, $\{k,i\}$, $\{i,l\}$, and $\{l,j\}$. For instance,

$$\boldsymbol{\omega}_{\{i,j\}}(x,y)\cdot(-c_{jk}, b_{jk}) = 0, \qquad (x,y)\in\{j,k\}$$

Moreover, along the edge $\{i,j\}$, as a limit value from inside the triangle T_{ijk} and from inside the triangle T_{ilj},

$$\boldsymbol{\omega}_{\{i,j\}}(x,y)\cdot(-c_{ji}, b_{ji}) = 1, \qquad (x,y)\in\{i,j\}$$

This implies that the tangential component of $\boldsymbol{\omega}_{\{i,j\}}$ is continuous and constant along $\{i,j\}$, and, furthermore, that the line integral of $\boldsymbol{\omega}_{\{i,j\}}$ along $\{i,j\}$ is one. To this end, on the edges the tangential components of the Whitney fields are continuous, and

$$\int_e \boldsymbol{\omega}_{e'}\cdot d\boldsymbol{l} = \delta_{e,e'} = \begin{cases}1, & e = e' \\ 0, & e \neq e'\end{cases} \tag{B.7}$$

where e and e' belong to the set of edges.

B.3 Some useful scalar products

Throughout this section, we assume that the relative permittivity $\epsilon(x, y)$ is real. Modifications due to a complex relative permittivity are straightforward, see Section B.1.

In this section, we calculate a number of scalar products of edge elements and gradients of node elements that appear in the main body of the text. Vector average values involving the edge elements are given also.

First, we wish to solve the integrals, see (3.5)

$$\begin{aligned} b_{\{i,j\};i} &= \iint_{\Omega_{\text{ext}}} \epsilon(x,y,z)\boldsymbol{\omega}_{\{i,j\}}(x,y)\cdot\nabla_{xy}\lambda_i(x,y)\,dx\,dy \\ &= \iint_{T_{ijk}} \frac{\phi_{ijk}(x,y)(b_{ki},c_{ki})-\phi_{jki}(x,y)(b_{jk},c_{jk})}{2\Delta_{ijk}}\cdot\frac{(b_{jk},c_{jk})}{2\Delta_{ijk}}\epsilon(x,y)\,dxdy \\ &+ \iint_{T_{ilj}} \frac{\phi_{ilj}(x,y)(b_{il},c_{il})-\phi_{jil}(x,y)(b_{lj},c_{lj})}{2\Delta_{ilj}}\cdot\frac{(b_{lj},c_{lj})}{2\Delta_{ilj}}\epsilon(x,y)\,dxdy \end{aligned}$$

and

$$\begin{aligned} b_{\{j,k\};i} &= \iint_{\Omega_{\text{ext}}} \epsilon(x,y,z)\boldsymbol{\omega}_{\{j,k\}}(x,y)\cdot\nabla_{xy}\lambda_i(x,y)\,dx\,dy \\ &= \iint_{T_{ijk}} \frac{\phi_{jki}(x,y)(b_{ij},c_{ij})-\phi_{kij}(x,y)(b_{ki},c_{ki})}{2\Delta_{ijk}}\cdot\frac{(b_{jk},c_{jk})}{2\Delta_{ijk}}\epsilon(x,y)\,dxdy \end{aligned}$$

where $\epsilon(x, y)$ is assumed to be (real and) continuous in T_{ijk} and in T_{ilj}, respectively. Here, the vector to the left of the dot represents a Whitney field of degree 1 and the vector to the right represents the gradient of a node element.

Using the mean value theorem (B.3) gives

$$\begin{aligned} b_{\{i,j\};i} =& \frac{1}{6}\frac{\epsilon_{ijk}(b_{ki},c_{ki})\cdot(b_{jk},c_{jk})-\epsilon_{jki}(b_{jk},c_{jk})\cdot(b_{jk},c_{jk})}{2\Delta_{ijk}} \\ &+\frac{1}{6}\frac{\epsilon_{ilj}(b_{il},c_{il})\cdot(b_{lj},c_{lj})-\epsilon_{jil}(b_{lj},c_{lj})\cdot(b_{lj},c_{lj})}{2\Delta_{ilj}} \end{aligned}$$

for some values ϵ_{ijk} and ϵ_{jki} of the permittivity in the triangle T_{ijk} and for some values ϵ_{ilj} and ϵ_{jil} of the permittivity in the triangle T_{ilj}. Similarly, one gets

$$b_{\{j,k\};i} = \frac{1}{6}\frac{\epsilon_{jki}(b_{ij},c_{ij})\cdot(b_{jk},c_{jk})-\epsilon_{kij}(b_{ki},c_{ki})\cdot(b_{jk},c_{jk})}{2\Delta_{ijk}}$$

for some values ϵ_{jki} and ϵ_{kij} of the permittivity in the triangle T_{ijk}.

There is also need for the integrals $b_{\{j,i\};i}$ and $b_{\{k,j\};i}$, which can be obtained from (B.6):

$$\begin{cases} b_{\{j,i\};i} = -b_{\{i,j\};i} \\ b_{\{k,j\};i} = -b_{\{j,k\};i} \end{cases}$$

Second, we wish to obtain the average values $<\epsilon(x,y)\boldsymbol{\omega}_{\{i,j\}}(x,y)>$, see Section 2.1. Using equations (B.3)–(B.5) yields

$$\begin{aligned}<\epsilon(x,y)\boldsymbol{\omega}_{\{i,j\}}(x,y)> &= \epsilon_{ijk}\frac{(b_{ki},c_{ki})}{6} - \epsilon_{jki}\frac{(b_{jk},c_{jk})}{6} \\ &+ \epsilon_{ilj}\frac{(b_{il},c_{il})}{6} - \epsilon_{jil}\frac{(b_{lj},c_{lj})}{6}\end{aligned}$$

for some values ϵ_{ijk} and ϵ_{jki} of the permittivity in the triangle T_{ijk} and for some values ϵ_{ilj} and ϵ_{jil} of the permittivity in the triangle T_{ilj}.

In practise, we approximate both the values ϵ_{ijk} and ϵ_{jki} by the average value of ϵ in T_{ijk}. We also use the formulae obtained for the real case in the complex case. These approximations are justified when the discretization is fine enough.

Appendix C Explicit formulae

The geometry that is appropriate in this paper implies that the "tent" function λ_i associated with node i can be written as (the super index 1, 2, 3, 4, 5, and 6 refer to the different areas of support depicted in Figure 10)

$$\lambda_i(x,y) = \phi_i^1(x,y) + \phi_i^2(x,y) + \phi_i^3(x,y) + \phi_i^4(x,y) + \phi_i^5(x,y) + \phi_i^6(x,y) \qquad \text{(C.1)}$$

where

$$\begin{cases} \phi_i^1(x,y) = \begin{cases} -\left(\dfrac{x-x_{i+1}}{x_{i+1}-x_i} - \dfrac{y-y_i}{y_i-y_{i-n}}\right), & (x,y)\in D_i^1 \\ 0, \quad \text{elsewhere} \end{cases} \\ \phi_i^2(x,y) = \begin{cases} -\dfrac{x-x_{i+1}}{x_{i+1}-x_i}, & (x,y)\in D_i^2 \\ 0, \quad \text{elsewhere} \end{cases} \\ \phi_i^3(x,y) = \begin{cases} -\dfrac{y-y_{i+n}}{y_{i+n}-y_i}, & (x,y)\in D_i^3 \\ 0, \quad \text{elsewhere} \end{cases} \end{cases}$$

$$\begin{cases} D_i^1 = \{(x,y) : x_i < x < x_{i+1},\ y_i + (y_i - y_{i-n})(x-x_{i+1})/(x_{i+1}-x_i) < y < y_i\} \\ D_i^2 = \{(x,y) : x_i < x < x_{i+1},\ y_i < y < y_i + (y_{i+n}-y_i)(x-x_i)/(x_{i+1}-x_i)\} \\ D_i^3 = \{(x,y) : x_i < x < x_{i+1},\ y_i + (y_{i+n}-y_i)(x-x_i)/(x_{i+1}-x_i) < y < y_{i+n}\} \end{cases}$$

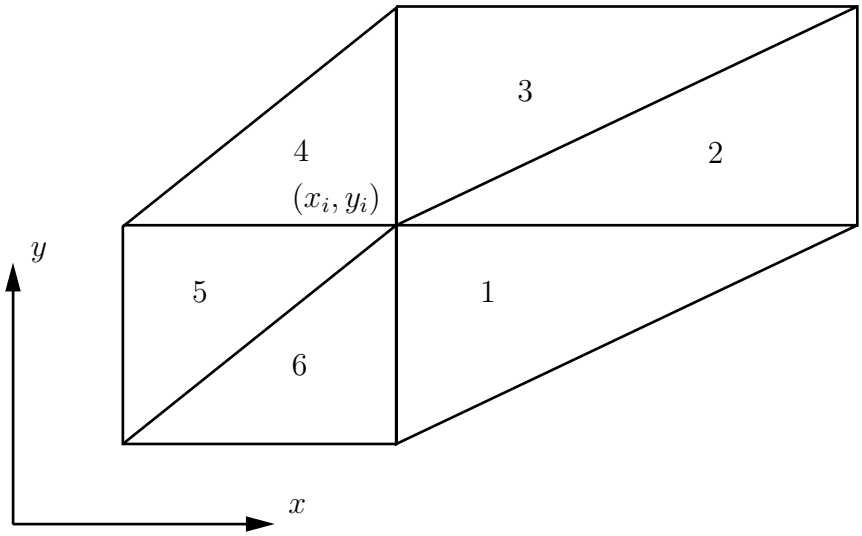

Figure 10: The support of the function $\lambda_i(x, y)$ and the different areas of the support of the functions $\phi_i^p(x, y)$, $p = 1, 2, 3, 4, 5, 6$.

and

$$\begin{cases} \phi_i^4(x,y) = \begin{cases} \dfrac{x - x_i}{x_i - x_{i-1}} - \dfrac{y - y_{i+n}}{y_{i+n} - y_i}, & (x,y) \in D_i^4 \\ 0, \quad \text{elsewhere} \end{cases} \\ \phi_i^5(x,y) = \begin{cases} \dfrac{x - x_{i-1}}{x_i - x_{i-1}}, & (x,y) \in D_i^5 \\ 0, \quad \text{elsewhere} \end{cases} \\ \phi_i^6(x,y) = \begin{cases} \dfrac{y - y_{i-n}}{y_i - y_{i-n}}, & (x,y) \in D_i^6 \\ 0, \quad \text{elsewhere} \end{cases} \end{cases}$$

$$\begin{cases} D_i^4 = \{(x,y) : x_{i-1} < x < x_i,\ y_i < y < y_i + (y_{i+n} - y_i)(x - x_{i-1})/(x_i - x_{i-1})\} \\ D_i^5 = \{(x,y) : x_{i-1} < x < x_i,\ y_i + (y_i - y_{i-n})(x - x_i)/(x_i - x_{i-1}) < y < y_i\} \\ D_i^6 = \{(x,y) : x_{i-1} < x < x_i,\ y_{i-n} < y < y_i + (y_i - y_{i-n})(x - x_i)/(x_i - x_{i-1})\} \end{cases}$$

The different areas of support of the functions $\phi_i^p(x, y)$, $p = 1, 2, 3, 4, 5, 6$ are depicted in Figure 10.

The gradient of the "tent" function about the interior node i is given by

$$\nabla_{xy}\lambda_i(x,y) = \begin{cases} -\left(\dfrac{\hat{\boldsymbol{x}}}{x_{i+1}-x_i} - \dfrac{\hat{\boldsymbol{y}}}{y_i - y_{i-n}}\right), & (x,y) \in D_i^1 \\ -\dfrac{\hat{\boldsymbol{x}}}{x_{i+1}-x_i}, & (x,y) \in D_i^2 \\ -\dfrac{\hat{\boldsymbol{y}}}{y_{i+n}-y_i}, & (x,y) \in D_i^3 \\ \dfrac{\hat{\boldsymbol{x}}}{x_i - x_{i-1}} - \dfrac{\hat{\boldsymbol{y}}}{y_{i+n}-y_i}, & (x,y) \in D_i^4 \\ \dfrac{\hat{\boldsymbol{x}}}{x_i - x_{i-1}}, & (x,y) \in D_i^5 \\ \dfrac{\hat{\boldsymbol{y}}}{y_i - y_{i-n}}, & (x,y) \in D_i^6 \\ \mathbf{0}, & \text{elsewhere} \end{cases}$$

The support of the edge element $\boldsymbol{\omega}_{\{i,j\}}$ coincides with the closure of the union of those triangular domains D_i^k that have the edge $\{i,j\}$ in common; specifically,

$$\begin{cases} \operatorname{supp}\left(\boldsymbol{\omega}_{\{i,i+1\}}\right) = \overline{D_i^1 \cup D_i^2} = \overline{D_{i+1}^4 \cup D_{i+1}^5} \\ \operatorname{supp}\left(\boldsymbol{\omega}_{\{i,i+1+n\}}\right) = \overline{D_i^2 \cup D_i^3} = \overline{D_{i+1+n}^5 \cup D_{i+1+n}^6} \\ \operatorname{supp}\left(\boldsymbol{\omega}_{\{i,i+n\}}\right) = \overline{D_i^3 \cup D_i^4} = \overline{D_{i+n}^6 \cup D_{i+n}^1} \end{cases}$$

In their supports, the basis functions are

$$\begin{cases} \boldsymbol{\omega}_{\{i,i+1\}} = \begin{cases} \dfrac{\hat{\boldsymbol{x}}}{x_{i+1}-x_i}\phi_i^1 + \left(\dfrac{\hat{\boldsymbol{x}}}{x_{i+1}-x_i} - \dfrac{\hat{\boldsymbol{y}}}{y_i - y_{i-n}}\right)\phi_{i+1}^5 & \text{in} \quad D_i^1 = D_{i+1}^5 \\ \left(\dfrac{\hat{\boldsymbol{x}}}{x_{i+1}-x_i} - \dfrac{\hat{\boldsymbol{y}}}{y_{i+n}-y_i}\right)\phi_i^2 + \dfrac{\hat{\boldsymbol{x}}}{x_{i+1}-x_i}\phi_{i+1}^4 & \text{in} \quad D_i^2 = D_{i+1}^4 \end{cases} \\ \boldsymbol{\omega}_{\{i,i+1+n\}} = \begin{cases} \dfrac{\hat{\boldsymbol{y}}}{y_{i+n}-y_i}\phi_i^2 + \dfrac{\hat{\boldsymbol{x}}}{x_{i+1}-x_i}\phi_{i+1+n}^6 & \text{in} \quad D_i^2 = D_{i+1+n}^6 \\ \dfrac{\hat{\boldsymbol{x}}}{x_{i+1}-x_i}\phi_i^3 + \dfrac{\hat{\boldsymbol{y}}}{y_{i+n}-y_i}\phi_{i+1+n}^5 & \text{in} \quad D_i^3 = D_{i+1+n}^5 \end{cases} \\ \boldsymbol{\omega}_{\{i,i+n\}} = \begin{cases} -\left(\dfrac{\hat{\boldsymbol{x}}}{x_{i+1}-x_i} - \dfrac{\hat{\boldsymbol{y}}}{y_{i+n}-y_i}\right)\phi_i^3 + \dfrac{\hat{\boldsymbol{y}}}{y_{i+n}-y_i}\phi_{i+n}^1 & \text{in} \quad D_i^3 = D_{i+n}^1 \\ \dfrac{\hat{\boldsymbol{y}}}{y_{i+n}-y_i}\phi_i^4 - \left(\dfrac{\hat{\boldsymbol{x}}}{x_i - x_{i-1}} - \dfrac{\hat{\boldsymbol{y}}}{y_{i+n}-y_i}\right)\phi_{i+n}^6 & \text{in} \quad D_i^4 = D_{i+n}^6 \end{cases} \end{cases}$$

The scalar products (3.5) are

$$\begin{cases}
b_{\{k,k+1\};k} = -\left\{(y_k - y_{k-n})/\left(x_{k+1} - x_k\right)/3 + (x_{k+1} - x_k)/\left(y_k - y_{k-n}\right)/6\right\}\epsilon(z, \boldsymbol{\xi}_k^1) \\
\qquad\qquad - (y_{k+n} - y_k)/\left(x_{k+1} - x_k\right)/3\epsilon(z, \boldsymbol{\xi}_k^2) \\
b_{\{k,k+1+n\};k} = -(y_{k+n} - y_k)/\left(x_{k+1} - x_k\right)/6\epsilon(z, \boldsymbol{\xi}_k^2) \\
\qquad\qquad - (x_{k+1} - x_k)/\left(y_{k+n} - y_k\right)/6\epsilon(z, \boldsymbol{\xi}_k^3) \\
b_{\{k,k+n\};k} = -(x_{k+1} - x_k)/\left(y_{k+n} - y_k\right)/3\epsilon(z, \boldsymbol{\xi}_k^3) \\
\qquad\qquad - \left\{(x_k - x_{k-1})/\left(y_{k+n} - y_k\right)/3 + (y_{k+n} - y_k)/\left(x_k - x_{k-1}\right)/6\right\}\epsilon(z, \boldsymbol{\xi}_k^4) \\
b_{\{k+1,k+1+n\};k} = (y_{k+n} - y_k)/\left(x_{k+1} - x_k\right)/6\epsilon(z, \boldsymbol{\xi}_k^2) \\
b_{\{k+n,k+1+n\};k} = (x_{k+1} - x_k)/\left(y_{k+n} - y_k\right)/6\epsilon(z, \boldsymbol{\xi}_k^3) \\
b_{\{k-1,k+n\};k} = \left\{(y_{k+n} - y_k)/\left(x_k - x_{k-1}\right)/6 - (x_k - x_{k-1})/\left(y_{k+n} - y_k\right)/6\right\}\epsilon(z, \boldsymbol{\xi}_k^4) \\
b_{\{k-1,k\};k} = (y_k - y_{k-n})/\left(x_k - x_{k-1}\right)/3\epsilon(z, \boldsymbol{\xi}_k^5) \\
\qquad\qquad + \left\{(y_{k+n} - y_k)/\left(x_k - x_{k-1}\right)/3 + (x_k - x_{k-1})/\left(y_{k+n} - y_k\right)/6\right\}\epsilon(z, \boldsymbol{\xi}_k^4) \\
b_{\{k-1-n,k-1\};k} = -(y_k - y_{k-n})/\left(x_k - x_{k-1}\right)/6\epsilon(z, \boldsymbol{\xi}_k^5) \\
b_{\{k-1-n,k\};k} = (x_k - x_{k-1})/\left(y_k - y_{k-n}\right)/6\epsilon(z, \boldsymbol{\xi}_k^6) \\
\qquad\qquad + (y_k - y_{k-n})/\left(x_k - x_{k-1}\right)/6\epsilon(z, \boldsymbol{\xi}_k^5) \\
b_{\{k-1-n,k-n\};k} = -(x_k - x_{k-1})/\left(y_k - y_{k-n}\right)/6\epsilon(z, \boldsymbol{\xi}_k^6) \\
b_{\{k-n,k\};k} = \left\{(y_k - y_{k-n})/\left(x_{k+1} - x_k\right)/6 + (x_{k+1} - x_k)/\left(y_k - y_{k-n}\right)/3\right\}\epsilon(z, \boldsymbol{\xi}_k^1) \\
\qquad\qquad + (x_k - x_{k-1})/\left(y_k - y_{k-n}\right)/3\epsilon(z, \boldsymbol{\xi}_k^6) \\
b_{\{k-n,k+1\};k} = \left\{(x_{k+1} - x_k)/\left(y_k - y_{k-n}\right)/6 - (y_k - y_{k-n})/\left(x_{k+1} - x_k\right)/6\right\}\epsilon(z, \boldsymbol{\xi}_k^1)
\end{cases}$$

for appropriate points $\boldsymbol{\xi}_k^l \in D_k^l$. In practise, average values of the permittivity are used in these expressions.

Explicit expressions for the average values $<\epsilon(z, \boldsymbol{\xi})>$ are needed also:

$$\begin{aligned}
<\epsilon(z, \boldsymbol{\xi})\boldsymbol{\omega}_{\{i,i+1\}}(\boldsymbol{\xi})> = &\epsilon(z, \boldsymbol{\xi}_i^1)\left(\hat{\boldsymbol{x}}\frac{y_i - y_{i-n}}{3} - \hat{\boldsymbol{y}}\frac{x_{i+1} - x_i}{6}\right) \\
&+\epsilon(z, \boldsymbol{\xi}_i^2)\left(\hat{\boldsymbol{x}}\frac{y_{i+n} - y_i}{3} - \hat{\boldsymbol{y}}\frac{x_{i+1} - x_i}{6}\right)
\end{aligned}$$

for some point $\boldsymbol{\xi}_i^1 \in D_i^1$ and some point $\boldsymbol{\xi}_i^2 \in D_i^2$,

$$<\epsilon(z, \boldsymbol{\xi})\boldsymbol{\omega}_{\{i,i+1+n\}}(\boldsymbol{\xi})> = \left(\epsilon(z, \boldsymbol{\xi}_i^2) + \epsilon(z, \boldsymbol{\xi}_i^3)\right)\left(\hat{\boldsymbol{x}}\frac{y_{i+n} - y_i}{6} + \hat{\boldsymbol{y}}\frac{x_{i+1} - x_i}{6}\right)$$

for some point $\boldsymbol{\xi}_i^2 \in D_i^2$ and some point $\boldsymbol{\xi}_i^3 \in D_i^3$, and

$$\begin{aligned}
<\epsilon(z, \boldsymbol{\xi})\boldsymbol{\omega}_{\{i,i+n\}}(\boldsymbol{\xi})> = &\epsilon(z, \boldsymbol{\xi}_i^3)\left(-\hat{\boldsymbol{x}}\frac{y_{i+n} - y_i}{6} + \hat{\boldsymbol{y}}\frac{x_{i+1} - x_i}{3}\right) \\
&+\epsilon(z, \boldsymbol{\xi}_i^4)\left(-\hat{\boldsymbol{x}}\frac{y_{i+n} - y_i}{6} + \hat{\boldsymbol{y}}\frac{x_i - x_{i-1}}{3}\right)
\end{aligned}$$

for some point $\boldsymbol{\xi}_i^3 \in D_i^3$ and some point $\boldsymbol{\xi}_i^4 \in D_i^4$. The average values $<\boldsymbol{\omega}_e(\boldsymbol{\xi})>$ are obtained by setting $\epsilon(z, \boldsymbol{\xi}) = 1$ in the above expressions for $<\epsilon(z, \boldsymbol{\xi})\boldsymbol{\omega}_e(\boldsymbol{\xi})>$.

Appendix D Some mathematical details

Introduce the weighted space $L^2_\epsilon(\mathbb{T})^2$ over the (two-dimensional) torus $\mathbb{T} \subset \mathbb{R}^3$:

$$L^2_\epsilon(\mathbb{T})^2 = \left\{ \boldsymbol{u} \in \mathbb{R}^2 \,\middle|\, \int_{\mathbb{T}} \epsilon(x)\, |\boldsymbol{u}(x)|^2 \, dS < \infty \right\}$$

where $\epsilon(x) > 0$ is a weighting function and dS is the surface element of the torus. In our example in this paper, the weight function $\epsilon(x)$ is the permittivity of the material. We also need differentiability (in the weak sense) of our functions. To this end, define

$$\mathbb{L} = L^2_\epsilon(\mathbb{T})^2 \cap H^1(\mathbb{T})^2$$

where $H^1(\mathbb{T})$ is the usual Sobolev space with weak partial derivatives on the torus.

Moreover, by the projection theorem we have the following orthogonal decomposition:

$$\mathbb{L} = \overline{\mathrm{Im}\,(\mathrm{Grad})} \oplus \mathrm{Im}\,(\mathrm{Grad})^\perp$$

where $\mathrm{Im}\,(\mathrm{Grad})$ is the space

$$\mathrm{Im}\,(\mathrm{Grad}) = \left\{ \boldsymbol{u} \in \mathbb{L} \,\middle|\, \boldsymbol{u} = \mathrm{Grad}\,\phi, \phi \in H^1(\mathbb{T}) \right\}$$

and Grad is the gradient defined on the torus.

The space $\mathrm{Im}\,(\mathrm{Grad})$ is a subset of the vector space $\mathrm{Ker}\,(\mathrm{Curl})$, which is defined as

$$\mathrm{Ker}\,(\mathrm{Curl}) = \{ \boldsymbol{u} \in \mathbb{L} \,|\mathrm{Curl}\,\boldsymbol{u} = \boldsymbol{0} \}$$

i.e.,

$$\overline{\mathrm{Im}\,(\mathrm{Grad})} \subset \mathrm{Ker}\,(\mathrm{Curl})$$

The operator Curl is the curl operator defined on the torus. If the underlying space is $\mathbb{R}^2$ we have $\overline{\mathrm{Im}\,(\mathrm{Grad})} = \mathrm{Ker}\,(\mathrm{Curl})$. The difference between the spaces we define as

$$\mathbb{H} = \mathrm{Ker}\,(\mathrm{Curl}) \cap \mathrm{Im}\,(\mathrm{Grad})^\perp$$

This space is characterized by

$$\mathrm{Curl}\,\boldsymbol{u} = \boldsymbol{0} \quad \text{and} \quad \int_{\mathbb{T}} \epsilon \boldsymbol{u} \cdot \nabla\phi \, dx = 0, \text{ for all } \phi \in H^1(\mathbb{T})$$

where, by Gauss' theorem on the torus (no boundary) is,

$$\int_{\mathbb{T}} \epsilon \boldsymbol{u} \cdot \nabla \phi \, dx = - \int_{\mathbb{T}} \mathrm{Div}\,(\epsilon \boldsymbol{u})\, \phi \, dx$$

The space $\mathbb{H}$ is therefore

$$\mathbb{H} = \{ \boldsymbol{u} \in \mathbb{L} \,|\mathrm{Curl}\, \boldsymbol{u} = \boldsymbol{0}, \mathrm{Div}\,(\epsilon \boldsymbol{u}) = 0 \}$$

where the derivatives are interpreted in the weak sense.

We notice that this space is exactly our basic equation, (2.7), rewritten in a slightly different notation. A modified version of Therorem D.1 given below, see [12, p. 219], then gives

$$\dim \mathbb{H} = 2 = B(\mathbb{T})$$

where $B(\mathbb{T})$ is the Betti-number of the torus.

Theorem D.1. *Let Ω be an open, bounded, and connected set in $\mathbb{R}^n$, $n = 2, 3$, with boundary Γ of class C^r, $r \geq 2$, of dimension $n-1$. The domain Ω is assumed to be locally situated on one side of Γ. Moreover, Γ has a finite number of connected components. Then the kernel of curl in $L^2(\Omega)^n$ is*

$$\begin{aligned} \mathcal{N}(\mathrm{curl}) &= \left\{ \boldsymbol{u} \in L^2(\Omega)^n, \mathrm{curl}\, \boldsymbol{u} = 0 \right\} \\ &= \mathrm{grad}\, H^1(\Omega) \oplus \mathbb{H}_1(\Omega) \end{aligned}$$

where

$$\mathbb{H}_1(\Omega) = \left\{ \boldsymbol{u} \in L^2(\Omega)^n, \mathrm{curl}\, \boldsymbol{u} = 0, \mathrm{div}\, \boldsymbol{u} = 0, \boldsymbol{u} \cdot \hat{\boldsymbol{\nu}} = 0 \right\}$$

and, moreover, $\dim \mathbb{H}_1(\Omega) = N =$ the Betti number.

References

[1] R. K. Agarwal and A. Dasgupta. Prediction of electrical properties of plain-weave fabric composites for printed wiring board design. *Journal of Electronic Packaging*, **115**, 219–224, 1993.

[2] T. M. Apostol. *Mathematical Analysis*. Addison-Wesley, Reading, MA, USA, 1957.

[3] A. Bensoussan, J. L. Lions, and G. Papanicolaou. *Asymptotic Analysis for Periodic Structures*. North-Holland, Amsterdam, 1978.

[4] M. Beren and N. Silnutzer. Effective electrical, thermal and magnetic properties of fiber reinforced materials. *J. Composite Materials*, **5**, 246–249, 1971.

[5] A. Bossavit. Edge-elements for scattering problems. *E.D.F. Bulletin de la Direction des Études et Recherches — Serie C, Mathematiques Informatique*, **43**(2), 175–191, 1989.

[6] A. Bossavit. Magnetostatic problems in multiply connected regions: some properties of the curl operator. *IEE Proc. A*, **135**(3), 179–187, 1988.

[7] A. Bossavit. Whitney forms: a class of finite elements for three-dimensional computations in electromagnetism. *IEE Proc. A*, **135**(8), 493–500, 1988.

[8] P. C. Clemmow. *The Plane Wave Spectrum Representation of Electromagnetic Fields*. Pergamon, New York, 1966.

[9] R. Coccioli, T. Itoh, G. Pelosi, and P. P. Silvester. Finite-element methods in microwaves: A selected bibliography. *IEEE Antennas and Propagation Magazine*, **38**(6), 34–48, 1996.

[10] A. Dasgupta and R. K. Agarwal. Orthotropic thermal conductivity of plain-weave fabric composites using a homogenization technique. *J. Composite Materials*, **26**(18), 2736–2758, 1992.

[11] A. Dasgupta, R. K. Agarwal, and S. M. Bhandarkar. Three-dimensional modeling of woven-fabric composites for effective thermo-mechanical and thermal properties. *Composites Science and Technology*, **56**, 209–223, 1996.

[12] R. Dautray and J.-L. Lions. *Mathematical Analysis and Numerical Methods for Science and Technology, Volume 3: Spectral Theory and Applications*. Springer-Verlag, Berlin Heidelberg, 1990.

[13] H. Flanders. *Differential Forms with Applications to the Physical Sciences*. Academic Press, New York, 1963.

[14] D. J. Kozakoff. *Analysis of Radome-Enclosed Antennas*. Artech House, Boston, London, 1997.

[15] E. F. Kuester and C. L. Holloway. Comparison of approximations for effective parameters of artificial dielectics. *IEEE Trans. Microwave Theory Tech.*, **38**(11), 1752–1755, 1990.

[16] E. F. Kuester and C. L. Holloway. A low-frequency model for wedge or pyramid absorber arrays—I: Theory. *IEEE Trans. Electromagn. Compatibility*, **36**(4), 300–306, 1994.

[17] E. F. Kuester and C. L. Holloway. A low-frequency model for wedge or pyramid absorber arrays—II: Computed and measured results. *IEEE Trans. Electromagn. Compatibility*, **36**(4), 307–313, 1994.

[18] J. B. Manges and Z. J. Cendes. A generalized tree-cotree gauge for magnetic field computation. *IEEE Trans. Magnetics*, **31**(3), 1342–1347, 1995.

[19] Q. G. Ning and T. W. Chou. A closed-form solution of the transverse effective thermal conductivity of woven fabric composites. *J. Composite Materials*, **29**(17), 2280–2294, 1995.

[20] Q. G. Ning and T. W. Chou. Closed-form solutions of the in-plane effective thermal conductivities of woven-fabric composites. *Composites Science and Technology*, **55**, 41–48, 1995.

[21] A. F. Peterson. Vector finite element formulation for scattering from two-dimensional heterogeneous bodies. *IEEE Trans. Antennas Propagat.*, **43**(3), 357–365, 1994.

[22] S. Rikte, G. Kristensson, and M. Andersson. Propagation in bianisotropic media—reflection and transmission. Technical Report LUTEDX/(TEAT-7067)/1–31/(1998), Lund Institute of Technology, Department of Electromagnetic Theory, P.O. Box 118, S-211 00 Lund, Sweden, 1998.

[23] E. Sanchez-Palencia. Comportements local et macroscopique d'un type de milieux physiques heterogenes. *Int. J. Eng. Sci.*, **12**, 331–351, 1974.

[24] E. Sanchez-Palencia. *Non-Homogeneous media and Vibration Theory*. Springer-Verlag, Berlin, 1980.

[25] D. Sun, J. Manges, X. Yuan, and Z. Cendes. Spurious modes in finite-element methods. *IEEE Antennas and Propagation Magazine*, **37**(5), 12–24, 1995.

[26] J. L. Volakis, A. Chatterjee, and L. C. Kempel. *Finite Element Method for Electromagnetics*. IEEE Press, New York, 1998.

[27] J. P. Webb. The finite-element method for finding modes of dielectric-loaded cavities. *IEEE Trans. Microwave Theory Tech.*, **33**(7), 635–639, 1985.

[28] J. P. Webb. Edge elements and what they can do for you. *IEEE Trans. Magnetics*, **29**(2), 1460–1465, 1993.